Multi-purpose high-throughput image analysis using CellProfiler

The power of Cellprofiler

Final report
Minor research project

Mark Wekking
2021

UMC Utrecht

Universiteit Utrecht

Abstract

The aim of this study was to investigate the flexibility of Cellprofiler. Cellprofiler is a platform that is designed to analyze real-life microscopy images. In this paper, we describe how Cellprofiler can be used to:

- ➢ Differentiate nuclei based on the cell type in primary cardiac tissue;
- ➢ Analyze nuclei size in primary cardiac tissue;
- ➢ Analyze the nuclear structure of LMNA KO- and KD-clones in an intestinal organoid model;
- ➢ Differentiate the polarization of membrane layers in intestinal organoids.

All the projects show how easy Cellprofiler can be. While on the other hand, the sky is the limit with Cellprofiler.

Introduction

Omics, a term to describe the quantification of huge amounts of data points within defined boundaries[1]. For example, genomics where form, structure, mapping of the genome is studied[2]. Or metabolic, which focuses on both identification and quantification of all metabolites in a body[3]. Each of these studies aims to measure and quantify small aspects of a giant process. With techniques like single-cell whole-genome sequencing, whereas the name suggests, the whole genome of a single cell can be sequenced within a day[4]. Gathering genomic data was never this easy. Although huge steps have been made in these forms of omics, imaging is still not fully usable in these forms of high throughput analysis. Even though Microscopes have gotten better over the years, with never seen before resolutions. With confocal microscopes, it is possible to stain exclusively DNA within cells with DAPI and observe DNA structure[5,6]. Once the cells have been stained and are under the microscope, the researcher picks a couple of representative spots. These spots can then be quantified by hand in software like ImageJ[7]. Or software like Ilastik can be used to use machine learning in order to segment images[8]. The downside of software such as these is that they still need the user to analyze the images by either. Whether it is all images by hand, as in ImageJ, or a small portion in order to train the algorithm, as in Ilastik. Although these techniques could be used with small sets of images. If an imaging technique called scanning is used, in which the whole surface is imaged, analyzing all images by hand is not feasible anymore. Both techniques don't show true high throughput capabilities needed in omics research. With this paper, a new generation of images analysis is shown, with the use of Cellprofiler. Cellprofiler is software designed for high-throughput, custom and easy, image analysis[9]. Here we show that Cellprofiler can be used to

- ➢ Differentiate nuclei based on the cell type in primary cardiac tissue;
- ➢ Analyze nuclei size in primary cardiac tissue[10];
- ➢ Analyze the nuclear structure of LMNA KO- and KD-clones in an intestinal organoid model[11];
- ➢ Differentiate the polarization of membrane layers in intestinal organoids.

In order to show the potential power of Cellprofiler.

Results

Using Cellprofiler4.0 with primary cardiac tissue images in order to differentiate nuclei of different cell types

background/method

The images used are generated by Christian Blok and commissioned by Jiayi Pei. The background of this research lies in the effects of the PLN-R14del mutation, in expressed genes of a human heart compared to healthy hearths[10]. Associated with the PLN-R14del is both arrhythmogenic cardiomyopathy (ACM) and dilated cardiomyopathy[12,13]. Dutch patient screenings show that this mutation is the cause of 12% and 15% of the cardiomyopathy cases[14]. Phospholamban (PLN) is a small peptide, with less than 150 amino acids is affected by this mutation. And regulates the calcium (Ca2+) pumps in the cardiac cells[15]. It specifically regulates ATP2A2. It is shown that PLN-R14del cardiac tissue is infiltrated with adipocytes, resulting in cardiomyocytes fully surrounded with adipocytes. This pattern of fat accumulation in cardiac cells is not unique to PLN-R14del cells. Mutations in the PKP2 or TNNT2 gene also show a comparable pattern of fat accumulation in adults[16,17].

This pattern of fat accumulation can also be observed in the cardiac tissue of young cardiomyopathy patients containing mutations in genes associated with fatty acid oxidation, such as HADHA[18]. Jiayi et al. with their research explored the role of epigenetic changes and their effects on cardiac tissue[10]. Within this research, they explored several candidates that might induce metabolic changes in cardiac tissue. The candidates ATP2A2, PLN, TNNI3, HADHA, PLIN4, ATP5F1A, PPARA, and KLF15 were all examined inside cardiac tissue, making use of immunofluorescence. In total 4 tissue samples are taken. 2 of PLN-R14del heart tissue (PLN1 and PLN2) and 2 healthy donor hearths (ctr1 and ctr2) are imaged under the Leica SP8X confocal microscope. The tissue is cut in 2 directions, both longitudinal (L) and transversal (T). Besides the 2 cutting directions, tissue is also collected from the subepicardial part of the heart (S). resulting in 4 tissue samples, cut in 3 different ways. Every sample was stained with DAPI in order to stain the nuclei and TNNI3 to stain the sarcomeres. On further investigation of the images, it was discovered that not all nuclei were surrounded with sarcomeres as one would expect. Some nuclei would float around (figure 1).

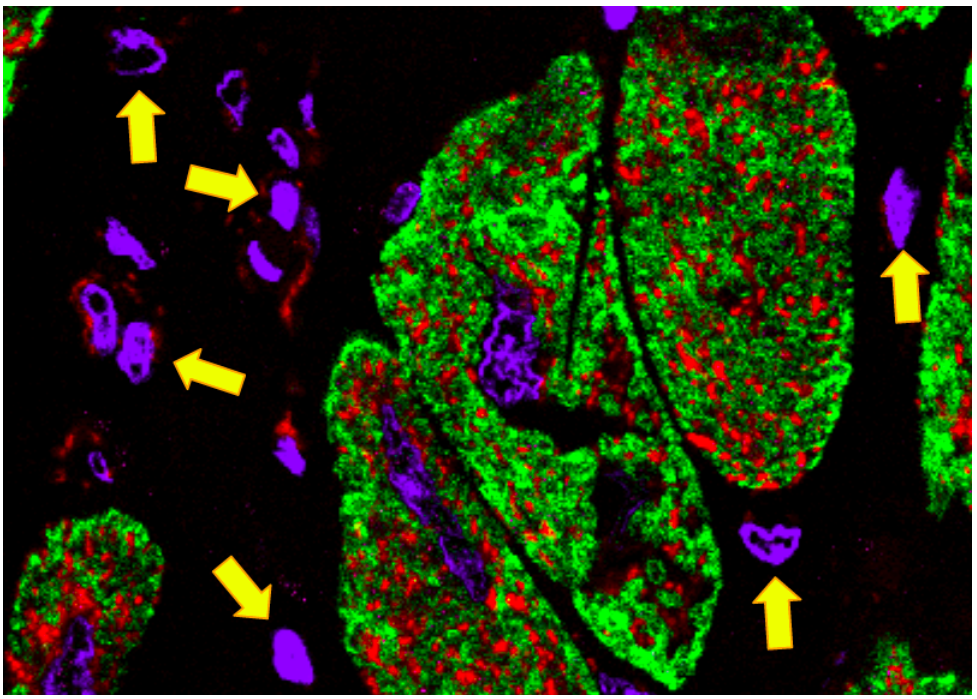

Figure 1. Showing stained cardiac tissue, in blue: DNA (DAPI), in green: sarcomeres (TNNI3), and in red: mitochondria (ATP5F1A)

Knowing that the cells filled with sarcomeres were cardiomyocytes, because of the other stainings also inside these cells, it was unclear to which cells these other nuclei belonged. Within this research, the goal is to generate a pipeline within Cellprofiler4.0 that can differentiate the nuclei belonging to the cardiomyocytes and the nuclei belonging to the unknown cells. Giving the option to use Cellprofiler4.0 to analyze 2 groups of the same cell type within the same images.

Method

The total Cellprofiler4.0 pipeline consists of 11 modules, not including the obligatory 4 starting modules (table 1.). The whole pipeline is divided into 3 parts, identifying the sarcomeres, identifying and quantifying 2 groups of nuclei based on the sarcomere location, preparing and saving final images, and varying features.

Table 1. schematic overview of the Cellprofiler4.0 pipeline from beginning to end.

Input	
	36 immunofluorescence cardiac tissue images were produced with the Leica SP8X confocal microscope. stained with 4 different stainings
Cellprofiler4.0 Modules	
Identifying sarcomeres	IdentifyPrimaryObjects
Identifying nuclei	MaskImage
Identifying nuclei	IdentifyPrimaryObjects
Identifying nuclei	MaskImage
Identifying nuclei	IdentifyPrimaryObjects
Preparing final images	GrayToColor
Preparing final images	DisplayDataOnImage
Preparing final images	DisplayDataOnImage
Preparing final images	SaveImages
Calculating final features	MeasureObjectSizeShape
Calculating final features	ExportToSpreadsheet
Downstream analysis	
	Custom Python script for Violin plot generation

Identifying sarcomeres

IdentifyPrimaryObjects

First, the sarcomeres are identified. For this, the IdentifyPrimaryObjects module is used with advanced settings. For some parameters the default settings of this module are used, only exemptions are listed. The typical diameter of the primary object lies between 1 and 10000 pixels, to ensure every pixel in the image is taken into account. Both objects outside the diameter range and touching the border are not discarded. For the intensity threshold, the threshold determining whether a pixel is on the foreground or background, the Otsu method is used. Three-class foreground thresholding was used. When using a two-class system, the threshold whether a pixel is a foreground or background is somewhere in the middle of the black to white scale (figure 2). While using a three-class thresholding method, the scale is divided into 3 parts, and in this case, the middle part will be seen as foreground (figure 2). This results in a more lenient selection. This method is used to ensure that all pixels belonging to the sarcomeres are identified and can be used to generate a mask.

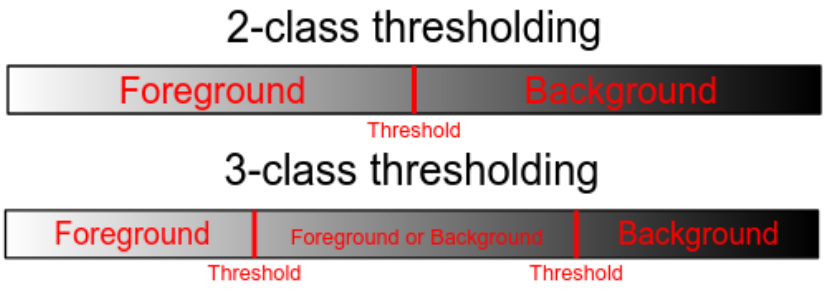

Figure 2. Showing the difference between 2-class and 3-class thresholding in Otsu thresholding. (Upper) Showing a 2-class division, with the threshold whether a pixel is a foreground or background lying somewhere in the middle. (lower) Showing a 3-class division, dividing the scale into 3 classes, and giving the user the choice if the middle part is either foreground or background.

The threshold correction factor is set to 0.1. With the Otsu thresholding method, it is inherently assumed approximately 50% of

the original image is covered with the foreground. Generally, the sarcomeres fill up more than 50% of the image (figure 3A). Sometimes the sarcomeres also contain holes that should be filled (figure 3B). Thus the thresholding factor needs to be lowered, signaling that probably more than 50% of the image is filled with objects (figure 3C). And no method for declumping is selected.

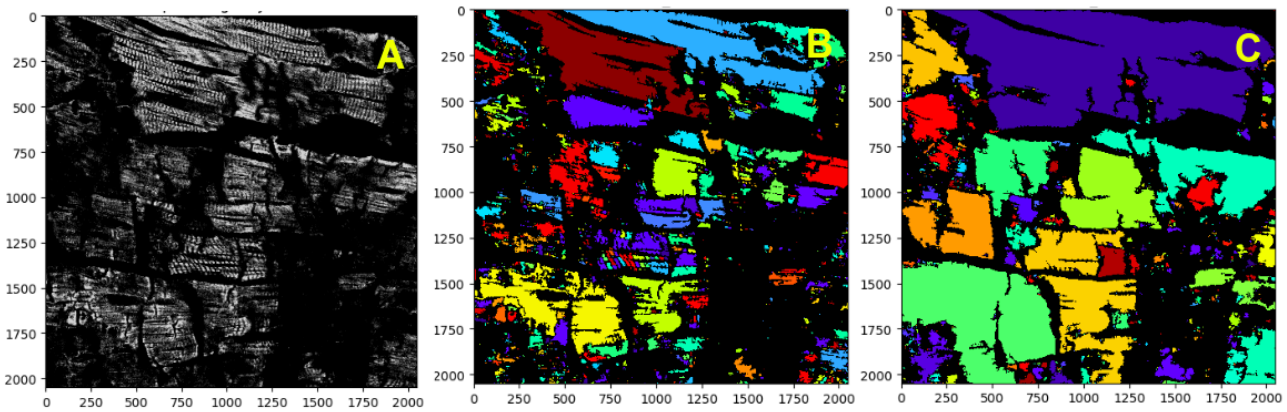

Figure 3. Showing the effects of changing the correction factor has on the objects Cellprofiler4.0 generates. (1A) Example of sacromere staining unprocessed. (1B) IdentifyPrimaryObjects, correction factor = 1.0. (1C) IdentifyPrimaryObjects, correction factor = 0.1

Differentiating nuclei types

MaskImage (unknown cells)

The MaskImage module can be used to mask certain areas. This is managed by setting the brightness value of each pixel in the selected area to 0 (image 4). The area masked out is indicated with the sarcomere object generated in the first IdentifyPrimaryObjects module. The mask is inverted, thus resulting in only the image outside of the sarcomere object. Thus all nuclei are in unknown cells.

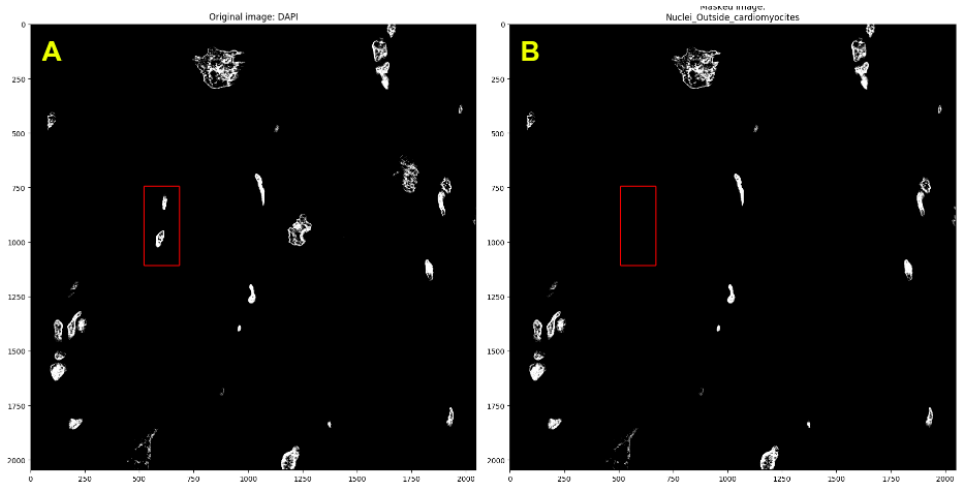

Figure 4. Showing stained nuclei before (A) and after masking all nuclei in cardiomyocytes (B).

IdentifyPrimaryObjects (unknown cells)

All unmasked nuclei are identified. These are the nuclei not in the cardiomyocytes. The IdentifyPrimaryObjects module is used with advanced settings. For some parameters the default settings of this module are used, only the exemptions are listed. The typical diameter of the nuclei is between 10 and 100 pixels. Objects touching the border are not discarded. Thresholding is done with the two-class Otsu method. The threshold factor is lowered to 0.7 to help the filling process of the nuclei (figure 5). Because the nuclei are generally separated from each other the declumping is set to none.

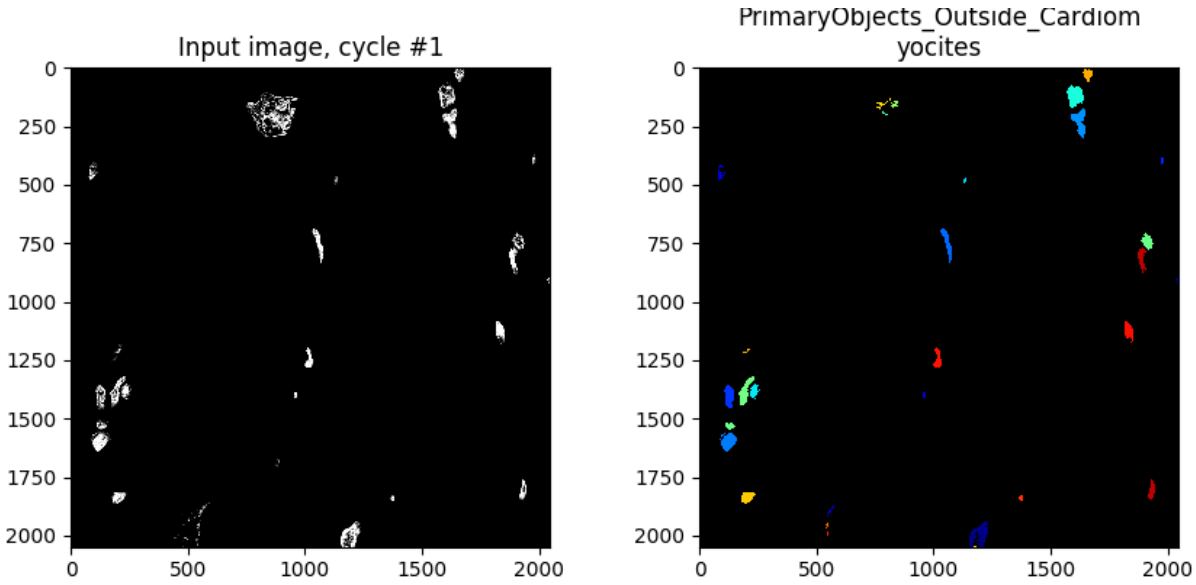

Figure 5. Showing the IdentifyPrimaryObjects module on the nuclei of unknown cells.

MaskImage (cardiomyocytes)

The area masked out is indicated with the sarcomere object generated in the first IdentifyPrimaryObjects module (figure 6). The mask is not inverted, resulting in only the image inside of the sarcomere object. Suggesting all nuclei are in cardiomyocytes.

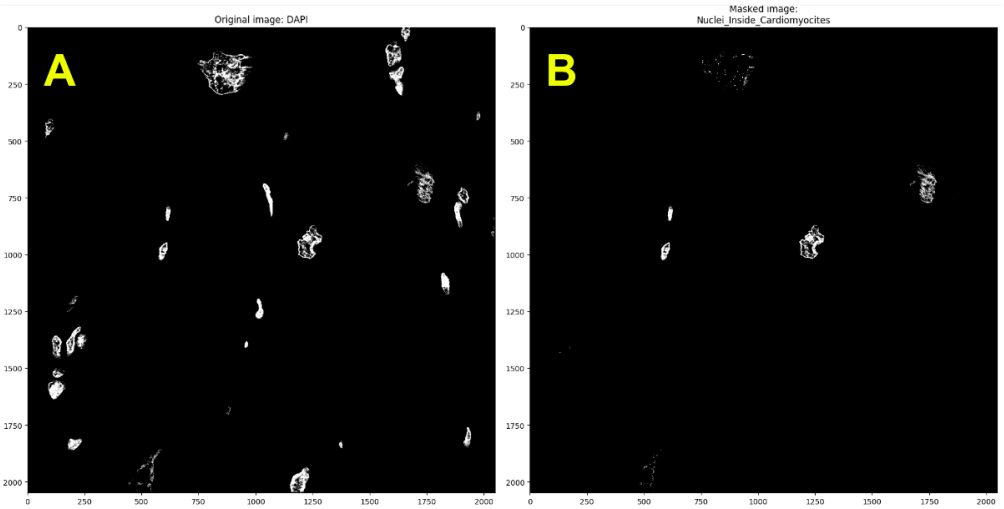

Figure 6. (A) Showing the original stained nuclei. (B) Showing stained nuclei after masking the sarcomeres.

IdentifyPrimaryObjects (cardiomyocytes)

All unmasked nuclei are identified. Because of the nature of the mask, these nuclei are inside the cardiomyocytes. IdentifyPrimaryObjects module is used with advanced settings. For some parameters the default settings of this module are used, only the exemptions are listed. The typical diameter of the nuclei is between 10 and 200 pixels. Objects touching the border are not discarded. Thresholding is done with a two-class Otsu method. with a correction factor of 0.1. No declumping is performed (figure 7).

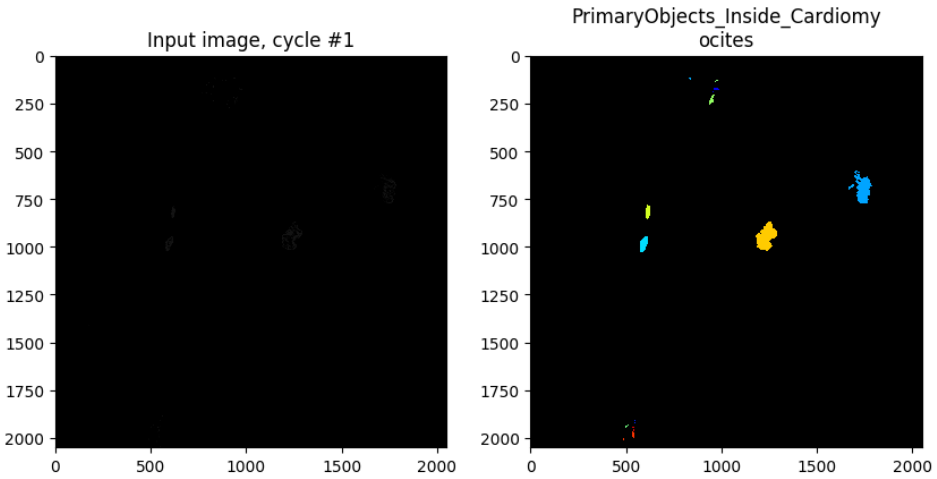

Figure 7. Showing the IdentifyPrimaryObjects module of the nuclei inside the cardiomyocytes.

Preparing final images

GrayToColor

The images are imaged per channel separately and loaded in a grayscale into Cellprofiler4.0. In order to generate a color image showing three of the four channels, the GrayToColor module is used (figure 8). Here channel 00 (DAPI), channel 02 (HADHA, PLN or ATP5F1A), and channel 03 (TNNI3) are used.

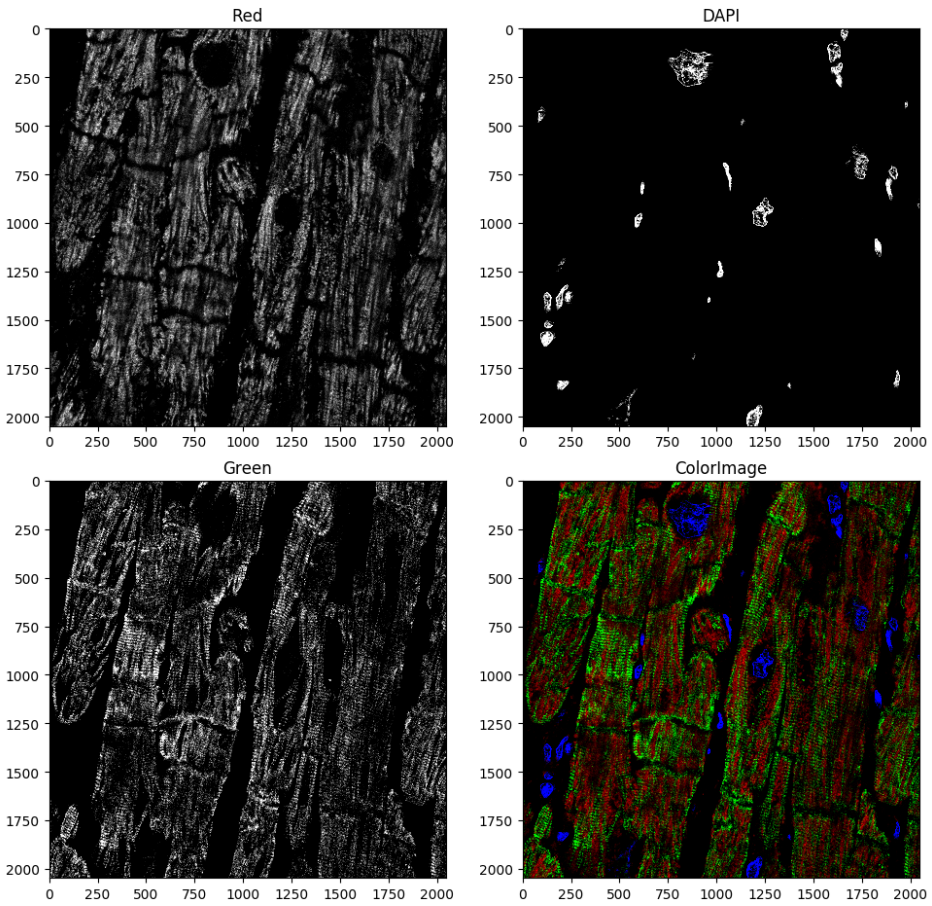

Figure 8. Showing the original channels in black and gray was used to generate the full-color image.

DisplayDataOnImage

This module is used in order to display any measurements as an overlay on an earlier image. It was used to display the number category, of the Object_number measurement, of the primary objects identified in the IdentifyPrimaryObjects module on top of the original image. The DisplayDataOnImage module was run twice, first for displaying the identified nuclei in the unknown cells and again for the nuclei inside the cardiomyocytes (figure 9).

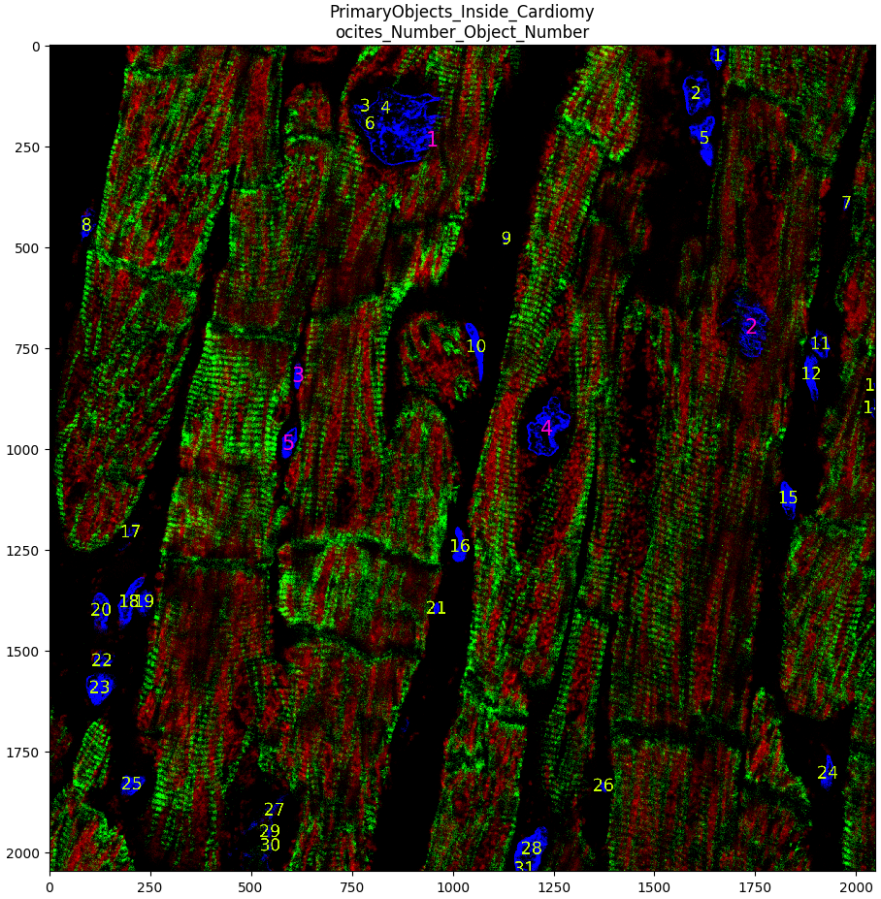

Figure 9. Showing the differentiated counted nuclei in the cardiomyocytes (magenta) and in unknown cells (yellow). In this tissue the nuclei are stained with DAPI (blue), PPARa is stained (not shown), ATP5F1A (red), and the sarcomeres with TNNI3 (green).

SaveImages

The produced images are saved in tiff format for every image set.

Calculating final features

MeasureObjectSizeShape

This module is used to measure several size and shape features of the earlier identified object of the IdentifyPrimaryObjects module. In default mode, applied to a 2D image, this module measures a total of 18 different features.

ExportToSpreadsheet

All measured features are exported to a comma-separated spreadsheet.

Downstream analysis

In order to compare the overall nucleus size a custom python script was used to export the data from the spreadsheet and visualize this in a violin plot.

results

The nucleus size of both the unknown cells and the cardiomyocytes is compared. In total 1095 nuclei belonging to unknown cells are identified. A total of 651 nuclei belonging to cardiomyocytes are identified. Overall the average nucleus size of cardiomyocytes is larger than those of the unknown cells. On average the nucleus size of cardiomyocytes in PLN-R14del cardiac tissue is larger than those of the healthy controls. Suggesting an increase in nucleus size in diseased tissue.

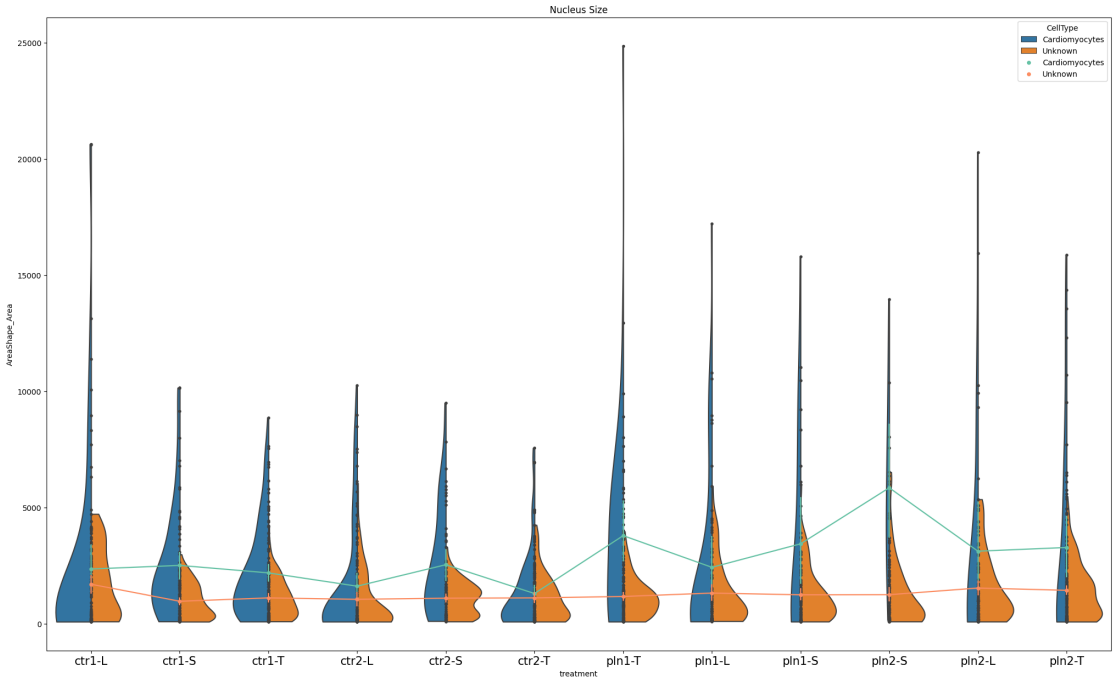

Figure 10. Violin plot showing nucleus size of both control and PLN-R14del cardiac tissue, comparing cardiomyocytes (blue) with unknown cells (orange)

Discussion

Cellprofiler4.0 was used to differentiate nuclei based on their cell type. This method of combining 2 stainings in order to differentiate

cell types can be used not only in cardiomyocytes but in other tissues or on other cells as well. This is based on the localization of the sarcomeres. Although this is a good indication of whether a cell is a cardiomyocyte or not, it is not a 100% guarantee. The sarcomeres could also lie in a different Z-stack which could result in the macromers not being fully visible. instead staining unique for cardiomyocytes would work better for this method. For example, a cardiac troponin staining. The downside is that the cardiac staining does not fill up the whole cell body. Besides the sarcomeres not being a failproof method of differentiating, the nuclei in the provided image set contained holes. these holes as seen in figure 9 in unknown nuclei 3,4,6 (yellow). These holes could have a couple of reasons. It could be that the staining didn’t fully work or that the image is taken in the wrong z-stack. Small holes can be filled up by adjusting the correction factor, but in this example, the hole is too big. Due to these holes, the IdentifyPrimaryObjects module has difficulties correctly identifying the nuclei as a single identity. Although this technique of combining 2 stainings is not fully failproof, with the right stainings and imaging it could be very useful in all kinds of stainings. Ali Nasser will continue on optimizing this pipeline in order to apply it to different tissue and cell types.

Using Cellprofiler4.0 together with an iPSC-cardiomyocyte model to analyze the effects of different growth media on nucleus size

background/method

The images used in this analysis were provided by Jiayi Pei and Renee Maas. Human cardiac induced pluripotent stem cells (iPSC) were seeded on a seahorse plate, in order to perform a seahorse assay. Here PLN iPSC-cardiomyocytes (D4) are compared to control iPSCs from a healthy donor (CVI-111). The original goal is to analyze the metabolic activity of the cells. The cells are grown on a high lipid medium, a high glucose medium, and a maturation growth medium. The aim of the Cellprofiler4.0 pipeline is to analyze the difference in nucleus growth. All nuclei are stained with a Hoechst staining. and imaged with a 20x magnification.

Method

The total Cellprofiler4.0 pipeline consists of 6 modules, not including the obligatory 4 starting modules (table 2). The goal of the pipeline is to identify and quantify the nuclei stained with a Hoechst staining and compare patients with control.

Table 2. Summarizing the image input into Cellprofiler, the Cellprofiler pipeline, and the downstream analysis performed on the output of Cellprofiler.

Input	
	60 immunofluorescence cardiac tissue image sets were produced with the Leica SP8X confocal microscope. stained with 3 different stainings
Cellprofiler4.0 modules	
	ColorToGray
	IdentifyPrimaryObjects

	DisplayDataOnImage
	SaveImages
	MeasureObjectSizeShape
	ExportToSpreadsheet
Downstream analysis	
	Custom python script for graph generation

ColorToGray

The images originally are in color but the Cellprofiler4.0 object identifier only works with grayscale images. Thus the images are converted to grayscale. Only the Hoechst staining is converted. The color splitting is based on the RGB model.

IdentifyPrimaryObjects

All stained nuclei are identified. IdentifyPrimaryObjects module is used with advanced settings. For some parameters the default settings of this module are used, only the exemptions are listed. The typical diameter of nuclei is between 30 and 150 pixels. Objects touching the border are discarded to exclude nuclei that are not completely imaged. These nuclei are left out because their object would not reflect the actual nucleus size, only a part of it. A global 3-class Otsu thresholding method is used. Pixels falling in the third class are seen as the background. Because there is a significant amount of nuclei not completely in focus and thus have a lower intensity (figure 11).

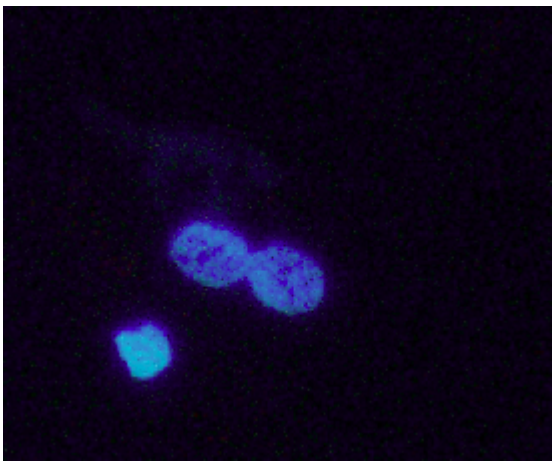

Image 11. showing 3 nuclei fully in focus, with a 4th nucleus out of focus and thus discarded as background.

The thresholding correction factor is set to 0.8. Both the method for distinguishing clumped objects and drawing separation lines between these objects are based on the shape of the object (figure 12).

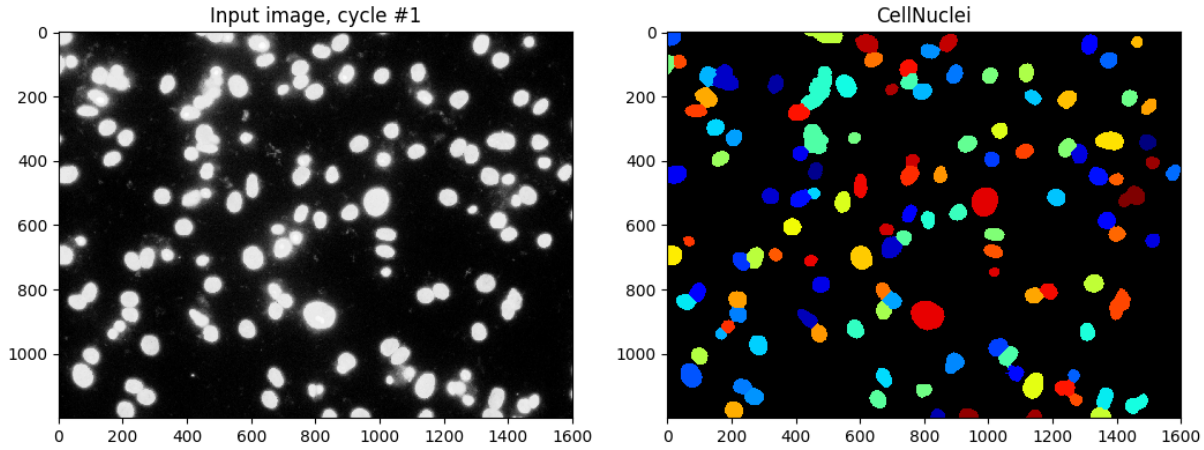

Figure 12. Showing an example of the IdentifyPrimaryObjects module

DisplayDataOnImage

This module is used in order to display any measurements as an overlay on an earlier image. It was used to display the number category, of the Object_number measurement, of the primary objects identified in the IdentifyPrimaryObjects module on top of the original image.

SaveImages

The produced images are saved in tiff format for every image set.

MeasureObjectSizeShape

This module is used to measure several size and shape features of the earlier identified object of the IdentifyPrimaryObjects module. In default mode, applied to a 2D image, this module measures a total of 18 different features.

ExportToSpreadsheet

All measured features are exported to a comma-separated spreadsheet.

results

The nucleus size of both D4 and CVI-111 are compared, within the same growth media. Here it can be seen that only in a high glucose environment the CVI-111 cells on average contain larger nuclei compared to the D4 cells (table 3, figure 13). In both the maturation medium and the lipid medium the D4 cells on average contain larger nuclei compared to the CVI-111 cells (table 3, figure 13). When comparing growth media, it is observed that in both maturation medium and lipid medium the D4 cell nuclei are on average larger (table 3, figure 13). With the maturation nuclei being the largest (table 3, figure 13). While in the CVI-111 cells, the nuclei in the maturation medium are on average the smallest (table 3, figure 13). The CVI-111 nuclei in the hg medium are the largest (table 3, figure 13).

	Hg	**Maturation**	**Lipid**
D4	2379	3019	3011
CVI-111	3014	2483	3009

Table 3. Showing the average nucleus size in pixels per sample group.

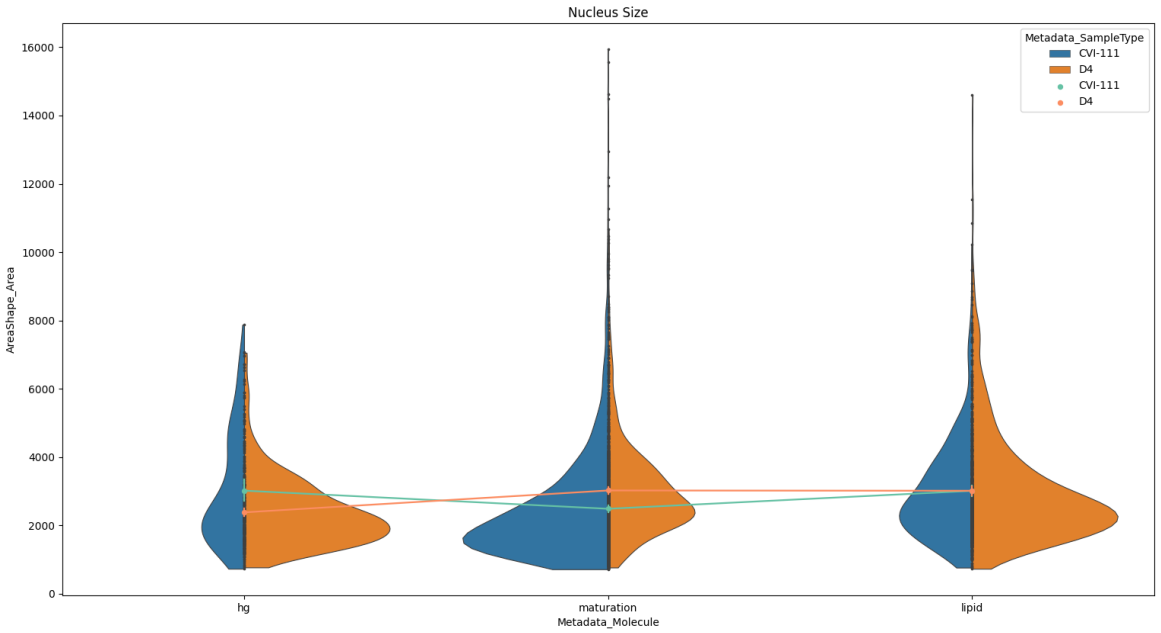

Figure 13. Violin graph showing the nucleus size (in pixels) of both D4 cells (orange) and CVI-111 cells (blue) grown on a high glucose medium (hg, left), a maturation medium (middle), and a lipid medium (right).

Discussion

Analyzing nucleus size can be a difficult process, taking up a large amount of time. This research shows the capabilities of Cellprofiler4.0 in fully automating this process. Thus taking away any subjectivity in measuring nuclei. Although Cellprofiler4.0 has some tools to remove nuclei that are in the background, these tools don't function without fault. Thus it is advised to limit the number of nuclei visible in a different z-stack as much as possible. The same goes for the declumping methods usable in Cellprofiler4.0. The declumping works, but is far from optimal. Thus it is advised to search for spots where the nuclei are not too clumped up. The seahorse assay shows an interesting view on the possible effects of growth media and how this affects the nucleus size and should definitely be investigated more. This project and this pipeline will be further used by Karen and Jiayi Pei in order to optimize the pipeline.

Using Cellprofiler4.0 with an intestinal organoid model in order to analyze the nuclear structure of LMNA KO and KD clones.

background

The original dataset was generated and provided by Bianca A. Meyer. The goal of the research was to generate *PKP2* and *LMNA* gene-edited primary intestinal organoids[11]. familial arrhythmogenic right ventricular (ARVC) is a form of cardiomyopathy that in many cases has been shown to be caused by mutations in a single gene[19]. Dutch patient screenings showed that a major group of familial ARVC is caused by mutations in the *PKP2 gene*[20]*.* While dilated cardiomyopathy in 5-10% of the cases is caused by a mutation in the *LMNA* gene[21]. In order to find potential drugs that can counter the effects of these mutations, organoids can be used[22]. Organoids are 3D cell structures, That mimic organ composition, that are patient-derived. Meaning that they display the same genetic properties as an individual. Making these structures ideal for the study of drug responses of patients. For the organoid generation, four different pathogenic variants have been selected[11]. 2 different variants for the *PKP2* mutation and 2 variants for the *LMNA* mutation. For each of these variants, one pegRNA was designed and cloned. These pegRNAs were used to transfect HEK293T cells together with a reported GFP-reporter plasmid to assess transfection efficiency. In the end, they managed to generate 3 *PKP2* and 3 *LMNA* knockout or knockdown intestinal organoid lines. After the generation of these knockout and knockdown organoid lines, a small group of organoids was stained with DAPI in order to investigate any nuclear morphology. Only *LMNA* organoids were stained because the *LMNA* gene plays a role in maintaining nuclear integrity, chromatin organization, and gene expression. Thus knocking such a gene out could result in significant morphological changes in the nuclear

structure. In total 24 images coming from 6 different groups, containing both patients and controls, were stained with DAPI, imaged with the Leica SP8X confocal microscope, and analyzed with Cellprofiler4.0[9]. Cellprofiler4.0 was used in order to investigate if the knocking-down or -out of *LMNA* in organoids has any effect on nuclear morphology.

methods

The total Cellprofiler4.0 pipeline consists of 8 modules, not including the obligatory 4 starting modules (table 4).

Table 4. table showing the whole pipeline from input images to downstream analysis.

Input	
	24 organoid images produced with the Leica SP8X confocal microscope
Cellprofiler4.0 Modules	
	ColorToGray
	Threshold
	MaskImage
	IdentifyPrimaryObjects
	DisplayDataOnImage
	SaveImages
	MeasureObjectSizeShape
	ExportToSpreadshet
Downstream analysis	
	Python script for: - Violin plot generation - Two sample student's t-test

ColorToGray

Cellprofiler4.0 is only capable of working with black and white images. Since the images are provided in color they have to be

converted to a black and white image. This is done with the *ColorToGray* module. Only a single channel was imaged, so only the blue channel was converted to gray (figure 14).

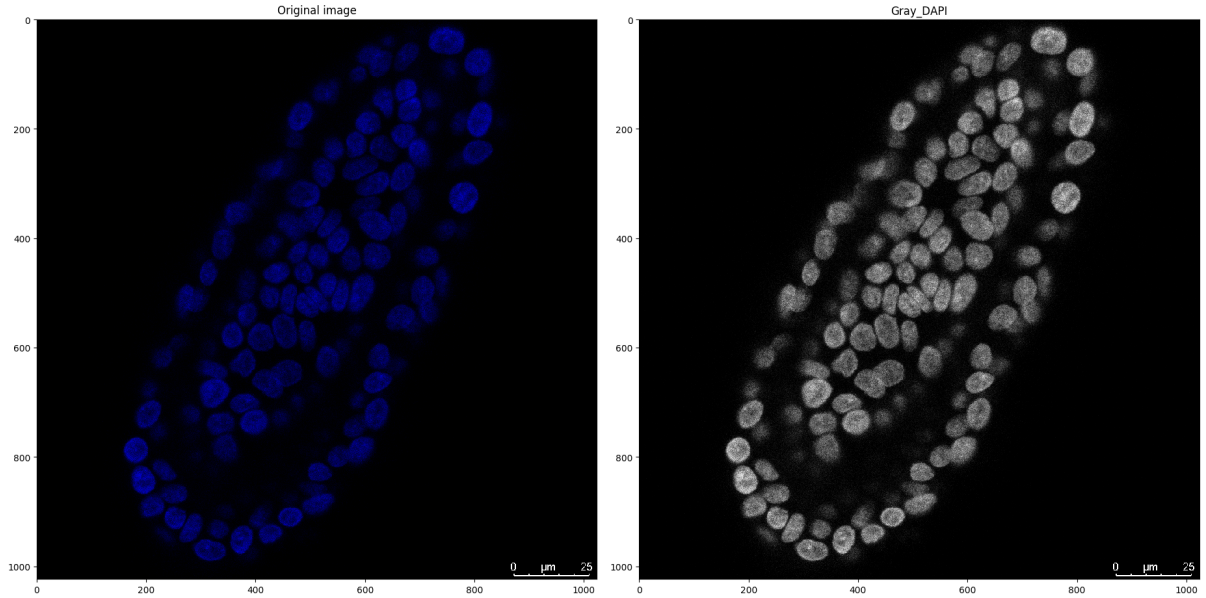

Figure 14. Showing the ColorToGray module On the left is the original color image. On the left is the image after converting the blue channel to a grayscale image.

Threshold

Every image has a scalebar in the lower right corner (figure 15).

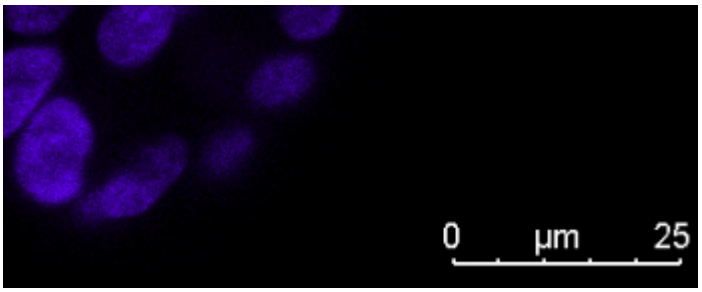

Figure 15. Image showing the scalebar present in every image.

This scalebar needs to be filtered out otherwise, Cellprofiler4.0 will detect these spots as possible cells. This is because Cellprofiler4.0 works by detecting lighter spots in darker areas. The Threshold module works by manually selecting a brightness, every pixel with a higher brightness gets marked. Because the brightness of every pixel is represented by a value between 0 and 1. And because the

scale bar is pure white, thus has a brightness value of 1. The threshold was set to 0.99, meaning that every pixel that has a brightness > 0.99 gets selected (figure 16).

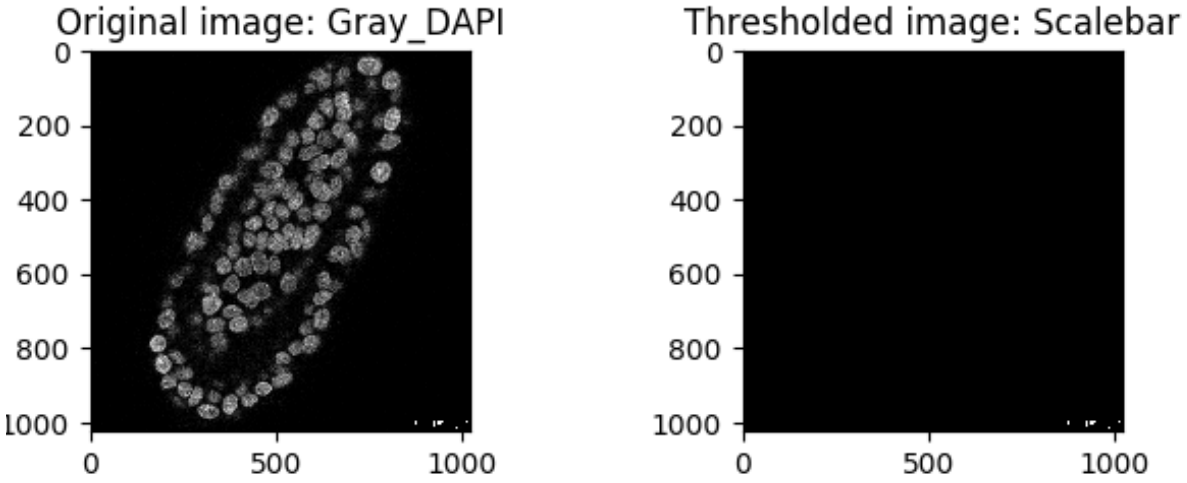

Figure 16. Image showing all pixels selected by the Threshold method. On the left is the image before Threshold. on the right are all pixels with a brightness value > 0.99 marked in white.

MaskImage

The MaskImage module can be used to mask certain areas. This is managed by setting the brightness value of each pixel in the selected area to 0 (figure 17). The masked area was indicated by the pixel selected in the threshold module.

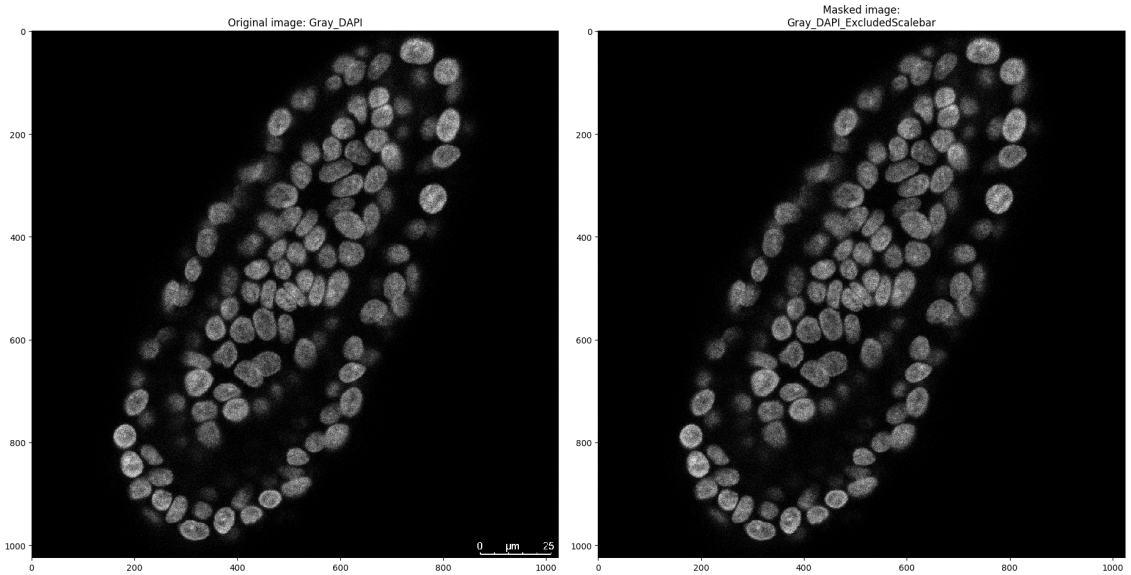

Figure 17. image showing the original image (left) and the image after removing the scalebar by masking it (right)

IdentifyPrimaryObjects

In this module, the nuclei are identified and counted (figure 18). The typical diameter of the objects is set to a minimum of 20 pixels and a maximum of 250 pixels. For the largest part, the default settings are used with some exemptions. Nuclei touching the border of the image are taken not discarded because, for the raw count of the nuclei, these nuclei are essential. The threshold for each image is calculated globally because the background in these images is mostly uniform. For the same reason, the Robust Background method was chosen as the thresholding method. 10% of the pixels with the lowest intensity are discarded because these pixels are most likely part of nuclei in a lower z-stack. The threshold correction factor was lowered to 0.8 in order to fill in gaps within the nuclei. Both the distinguishing and drawing lines between clumps are based on the shape of the nuclei. Because most nuclei in these organoids have fairly predictable shapes.

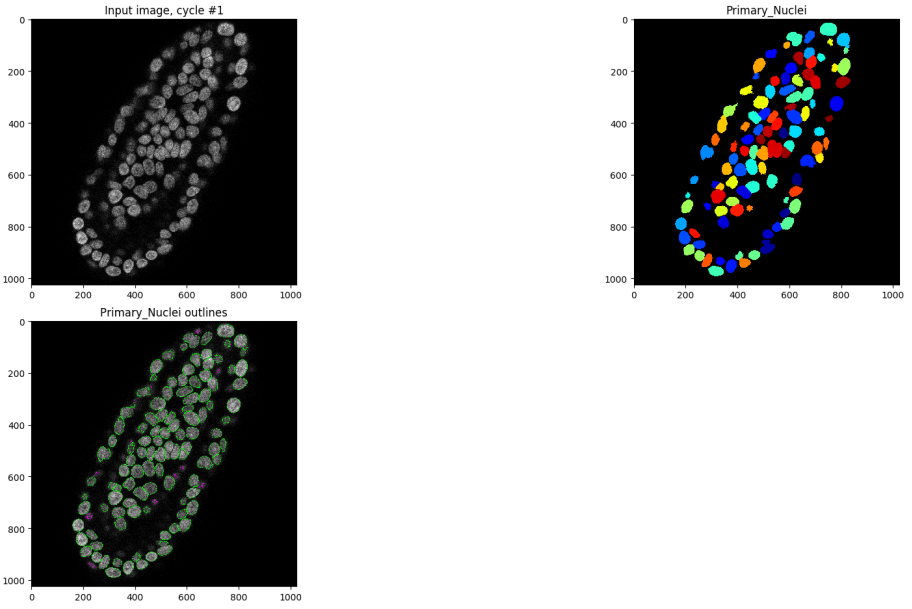

Figure 18. Showing the IdentifyPrimaryObject module. The top left, showing the original image. The lower left, showing the borders of objects Cellprofiler4.0 has identified. The top right shows the declumping of found objects and identifying them as unique objects.

DisplayDataOnImage

This module is used in order to display any measurements as an overlay on an earlier image. It was used to display the number category, of the Object_number measurement, of the primary objects identified in the IdentifyPrimaryObjects module on top of the original image (figure 19).

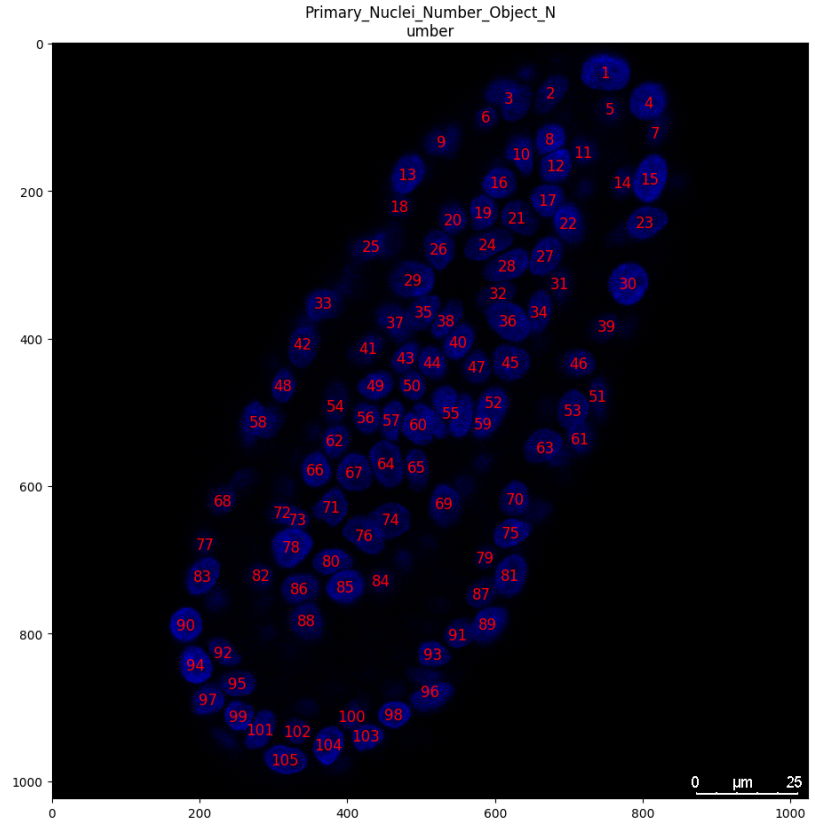

Figure 19. Showing the output of the DisplayDataOnImage module. The original microscopy image overlayed with the nuclei counts Cellprofiler quantified.

SaveImages

This module was used to save the image generated in the DisplayDataOnImage module.

MeasureObjectSizeShape

This module is used to measure several size and shape features of the earlier identified object of the IdentifyPrimaryObjects module. In default mode, applied to a 2D image, this module measures a total

of 18 different features.

ExportToSpreadsheet

Here all measurements made in earlier modules (IdentifyPrimaryObjects & MeasureObjectSizeShape) are converted to a comma-separated spreadsheet. For each nucleus found, all features are separately noted and ready for downstream analysis.

results

In total 3 control groups, 2 knockout groups, and 1 knockdown group are compared. The first control is a primary intestinal organoid, derived from a healthy donor, this is STE030. 4 images are taken, it should be noted that the digital zoom in the 4 images is not equal, it varies from 0.97 to 2.65 (Table 5). This may alter the results in the end. These variations in digital zoom are in all image sets. In total 329 nuclei were identified. The other 2 control groups 5-12 and 5-14 are healthy organoids that are transfected with empty plasmids. This is done in order to check if the transfection has any influence on organoid growth. 5 images from the 5-12 are supplied, resulting in 515 unique nuclei (Table 5). From the control group 5-14, 4 images are made which resulted in a total of 124 nuclei (Table 5). Apart from the control groups, 2 knockout organoids are stained. the first is 5-4, an *LMNA* knockout. 3 images are made, resulting in 469 nuclei (Table 5). 3 images from the 5-8 *LMNA* knockout are provided, resulting in 169 nuclei (Table 5). The last group is 5-5, this is the *LMNA* knockdown. There are 5 images from this group, which resulted in 125 nuclei (Table 5).

Table 5. Showing all groups used in the *LMNA* experiment. total of 6 groups, 3 control, 2 knockouts, 1 knockdown. For each group the total number of images is shown and the number of identified nuclei.

Name	**STE030**	**5-12**	**5-14**	**5-4**	**5-8**	**5-5**
Group	Control	Control	Control	Knockout	Knockout	Knockdown
No. images	4	5	4	3	3	5
Identified nuclei	329	515	124	469	169	125

Although the provided images show different levels of digital zoom, resulting in different nuclei sizes. These differences provide no problem for the quantification of different nuclei. The software is fully capable of distinguishing smaller nuclei from larger ones (figure 20). These differences in zoom only provide difficulties when metrics are analyzed that are based on a pixel count. For example the nucleus area size.

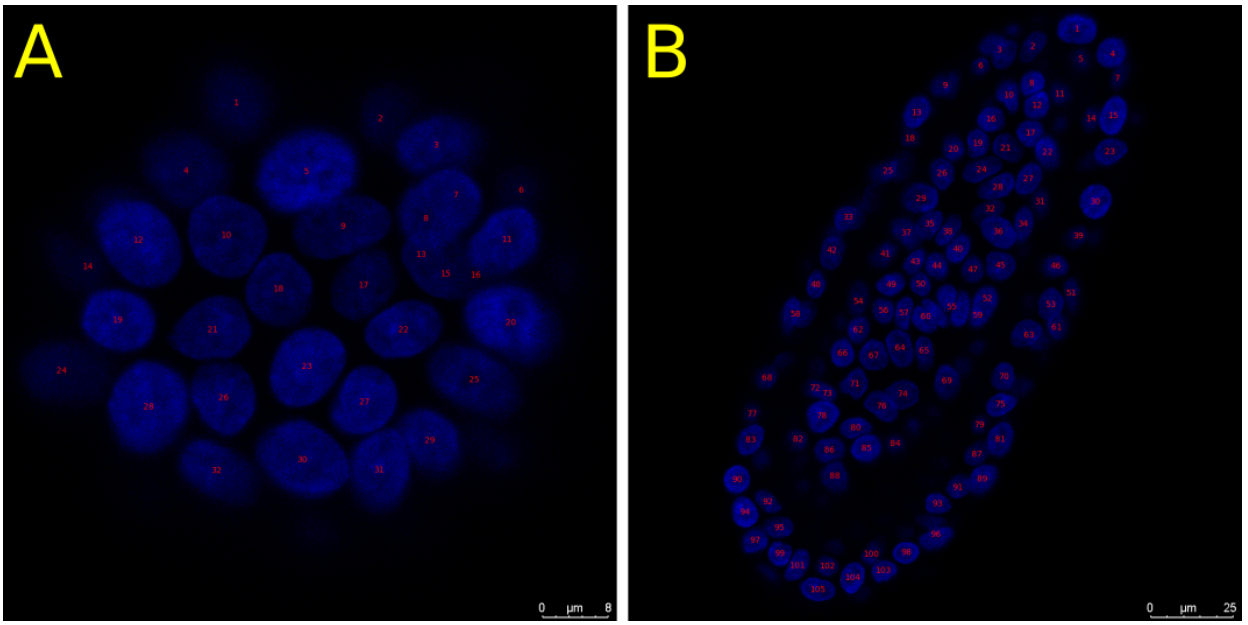

Figure 20. DAPI staining of healthy control organoids (STE030) overlayed with nuclei counts provided by Cellprofiler4.0 showing different digital zoom levels. (A). STE030 image 3, digital zoom level 2.65. **(B).** STE030 image 4, digital zoom level 1.00.

In total 18 different characteristics of the identified nuclei are measured. These measurements are then plotted to violin plots with

a custom python script, to give a clear overview of the data (Figure 21).

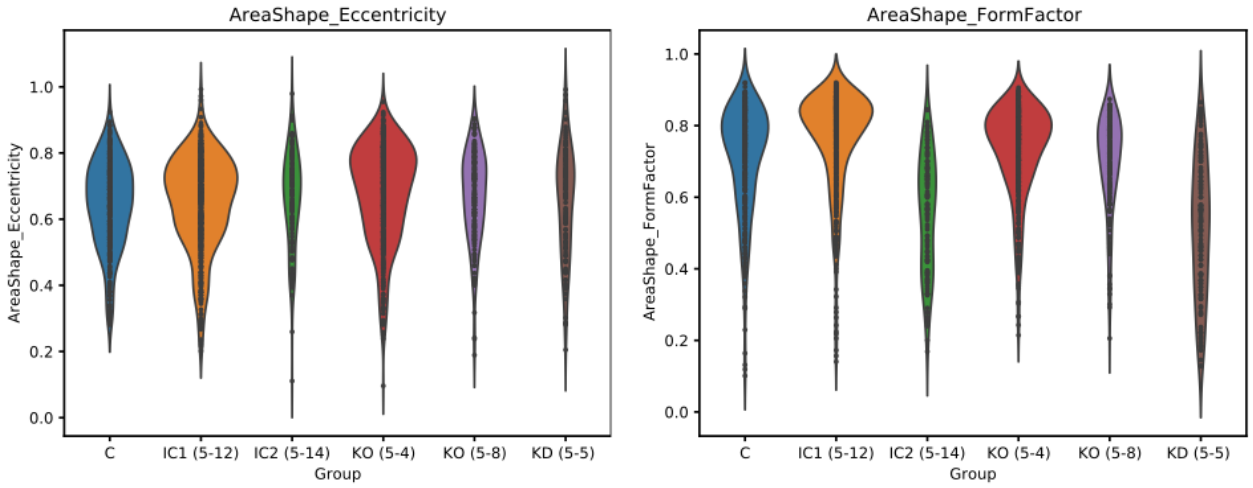

Figure 21. Two examples of figures that can be extracted from the spreadsheet exported by Cellprofiler4.0

Each characteristic is statistically checked for any significant differences between groups. This is done via a two-sample student's t-test (see supplementary table 1). In total 35 features had a significant difference between at least 1 control and 1 knockout or knockdown group (Table 6).

Table Table 6. Showing features with a significant difference between means, in controls and either KO- or KD- organoids (P>0.05).

Feature	Group1	group2	pvalue
AreaShape_MedianRadius	KO (5-8)	IC2 (5-14)	0,758
AreaShape_FormFactor	KO (5-8)	C (STE030)	0,355
AreaShape_Compactness	KO (5-8)	C (STE030)	0,679
AreaShape_Compactness	KO (5-4)	IC1 (5-12)	0,303
AreaShape_Eccentricity	KO (5-8)	IC2 (5-14)	0,620
AreaShape_Eccentricity	KO (5-8)	KO (5-4)	0,455
AreaShape_Eccentricity	KO (5-8)	KD (5-5)	0,383
AreaShape_Eccentricity	KO (5-8)	IC1 (5-12)	0,123
AreaShape_Eccentricity	IC2 (5-14)	KO (5-4)	0,222
AreaShape_Eccentricity	IC2 (5-14)	C (STE030)	0,229
AreaShape_Eccentricity	IC2 (5-14)	KD (5-5)	0,719
AreaShape_Eccentricity	IC2 (5-14)	IC1 (5-12)	0,442

AreaShape_Eccentricity	KO (5-4)	KD (5-5)	0,969
AreaShape_Eccentricity	C (STE030)	KD (5-5)	0,493
AreaShape_Eccentricity	C (STE030)	IC1 (5-12)	0,515
AreaShape_Eccentricity	KD (5-5)	IC1 (5-12)	0,790
AreaShape_Solidity	KO (5-8)	KO (5-4)	0,929
AreaShape_Solidity	KO (5-8)	C (STE030)	0,350
AreaShape_Solidity	IC2 (5-14)	KD (5-5)	0,520
AreaShape_Solidity	KO (5-4)	C (STE030)	0,199
AreaShape_Extent	KO (5-8)	IC2 (5-14)	0,282
AreaShape_Extent	KO (5-8)	KO (5-4)	0,784
AreaShape_Extent	KO (5-8)	C (STE030)	0,104
AreaShape_Extent	KO (5-4)	C (STE030)	0,934
AreaShape_Orientation	KO (5-8)	IC2 (5-14)	0,727
AreaShape_Orientation	KO (5-8)	KO (5-4)	0,243
AreaShape_Orientation	KO (5-8)	C (STE030)	0,443
AreaShape_Orientation	KO (5-8)	IC1 (5-12)	0,966
AreaShape_Orientation	IC2 (5-14)	KO (5-4)	0,163
AreaShape_Orientation	IC2 (5-14)	C (STE030)	0,762
AreaShape_Orientation	IC2 (5-14)	IC1 (5-12)	0,742
AreaShape_Orientation	KO (5-4)	KD (5-5)	0,227
AreaShape_Orientation	KO (5-4)	IC1 (5-12)	0,107
AreaShape_Orientation	C (STE030)	IC1 (5-12)	0,368

Discussion

Cellprofiler4.0 is fully capable of distinguishing large amounts of nuclei. The fact that this large group of images were all in a different zoom, and thus had a huge fluctuation in nuclei size, was no problem at all for the software. The whole pipeline is easy to run locally but can also without a problem be used on Galaxy. A large downside is that there is no module that can be used to detect small irregularities in the nucleus form. Such as the dents that have been found in the Knockout treatment. In theory, it would be great if something comparable to the Boundingbox could be used. A circle around each individual object, which is a certain percentage bigger than the original. From there one could calculate how much of a percentage the outer wall of the nucleus takes in. This shows even though the pipeline is fully working, it still can be improved. The

project will continue and be done by Karen Gaar-Humphreys and Maaike de Vries.

Using Cellprofiler4.0 in combination with intestinal organoids in order to differentiate organoids based on the polarization of the membrane layers

background/method

The original dataset was generated and provided by Zahra Shojaeijeshvaghani and Maaike de Vries. With this research, the apical and basolateral polarization in intestinal organoids was examined. Normally the polarization of intestinal organoids is characterized by the expression of a6-integrin. Integrin is in normal situations, a cell surface protein. Thus the integrins are expressed in the basolateral layer of the organoids (figure 22). While filamentous-actin (F-actin), in normal cells, shows more apical expression and is more expressed in the lumen of the organoids (figure 22).

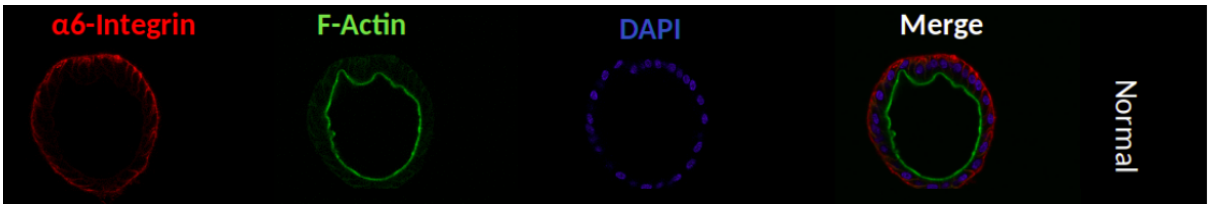

Figure 22. Showing the normal expression of a6-integrin, F-actin, and DNA (DAPI) in organoids. The a6-integrin is expressed on the outer membrane while the F-actin lines more of the lumen.

While normal intestinal organoids are characterized by the a6-integrin expression on the outside of the F-actin ring. Due to certain mutations, this normal polarization could change. The polarization of these organoids could invert, which could lead to inflammations. Organoids with an inverted polarity is marked by their F-actin expression on the outer membrane of the organoids.

While a6-integrin in these organoids is within the F-actin ring (Figure 23).

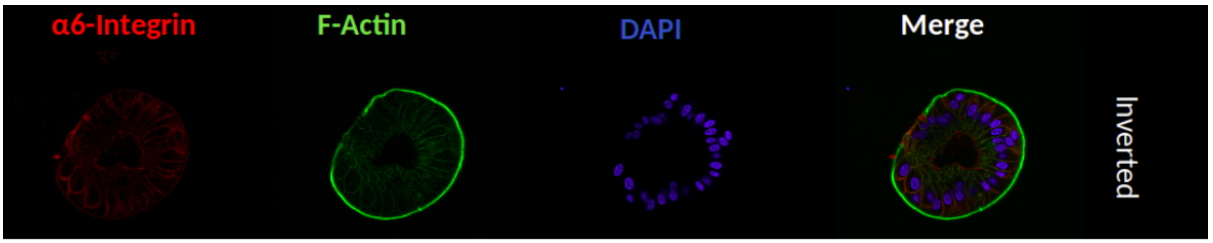

Figure 23. Showing the expression of a6-integrin, F-actin, and DNA (DAPI) within organoids with inverted polarity. The F-actin is expressed on the outer membrane of the organoids and the a6-integrin is contained within the F-actin ring.

The goal was to use Cellprofiler4.0 to distinguish between normal and inverted intestinal organoids. And use the software to quantify these normal and inverted organoids.

Methods

The total Cellprofiler4.0 pipeline consists of 16 modules, not including the obligatory 4 starting modules (table 7). The whole pipeline consists of 3 large parts. The pre-processing of the images, resizing the images and adjusting the intensity. The quantification of both normal and inverted organoids. And, image generation showing the quantification results.

Table 7. Showing the full pipeline used to distinguish between normal and inverted intestinal organoids.

Input	
	5 intestinal organoid image sets were produced with the Leica SP8X confocal microscope
Cellprofiler4.0 modules	
Pre-processing	GrayToColor
Pre-processing	Resize
Pre-processing	RescaleItensity

Pre-processing	Resize
Pre-processing	RescaleIntensity
Quantification of organoids	IdentifyPrimaryObjects
Quantification of organoids	ExpandOrShrinkObjects
Quantification of organoids	MaskImages
Quantification of organoids	IdentifyPrimaryObjects
Quantification of organoids	ExpandOrShrinkObjects
Quantification of organoids	MaskImages
Quantification of organoids	IdentifyPrimaryObjects
Quantification of organoids	Resize
Result image generation	DisplayDataOnImages
Result image generation	DisplayDataOnImages
Result image generation	SaveImages

Pre-processing

GrayToColor

The images are imaged per channel separately and loaded in a grayscale into Cellprofiler4.0. In order to generate a color image showing all three channels overlapping the GrayToColor module is used (figure 24). Here channel 00 (DAPI), channel 01 (a6-integrin), and channel 02 (F-actin) are used. It is clearly shown that the intensity of these images is really low.

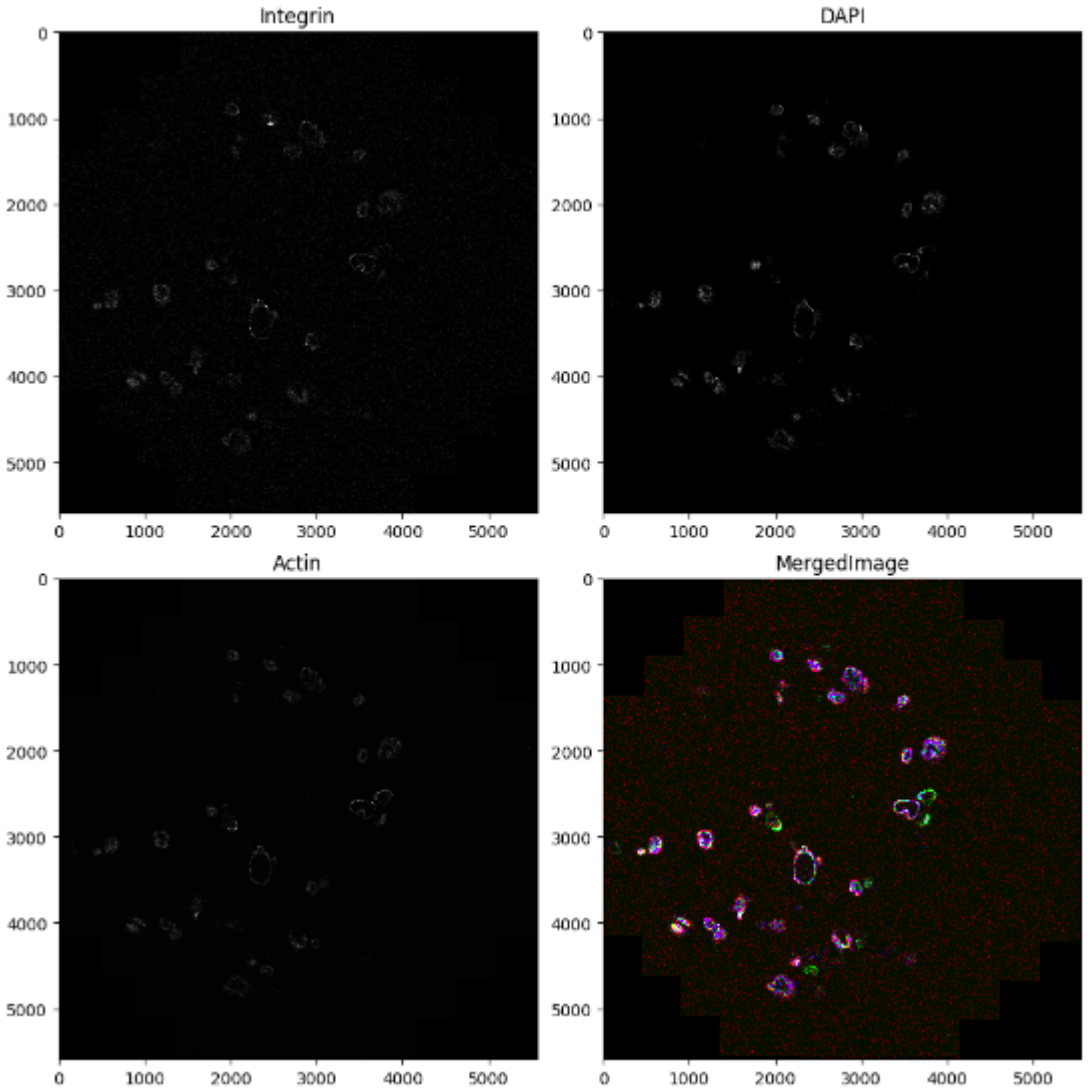

Figure 24. showing the GrayToColor module. The top left shows the DAPI staining, the top right shows the a6-integrin staining, the bottom left shows the F-actin staining, and the bottom right shows the merged color image. Both the contrast and the brightness of the merged image are increased post generation.

Resize

Because of the huge resolution of the original images, the image needs to be rescaled. This is done in order to contain memory usage as much as possible. Both the a6-integrin (ch01) and the F-actin (ch02) images are shrunken to 25% of their original size.

RescaleItensity

Because the original image intensity was too low for Cellprofiler4.0 to make a clear distinguishment between fore- and background, the

intensity is rescaled. The intensity of the actin image (figure 25A) is increased by a factor of 6.66 (Figure 25B). While the intensity of the a6-integrin (figure 25C) is increased by a factor of 20 (figure 25D).

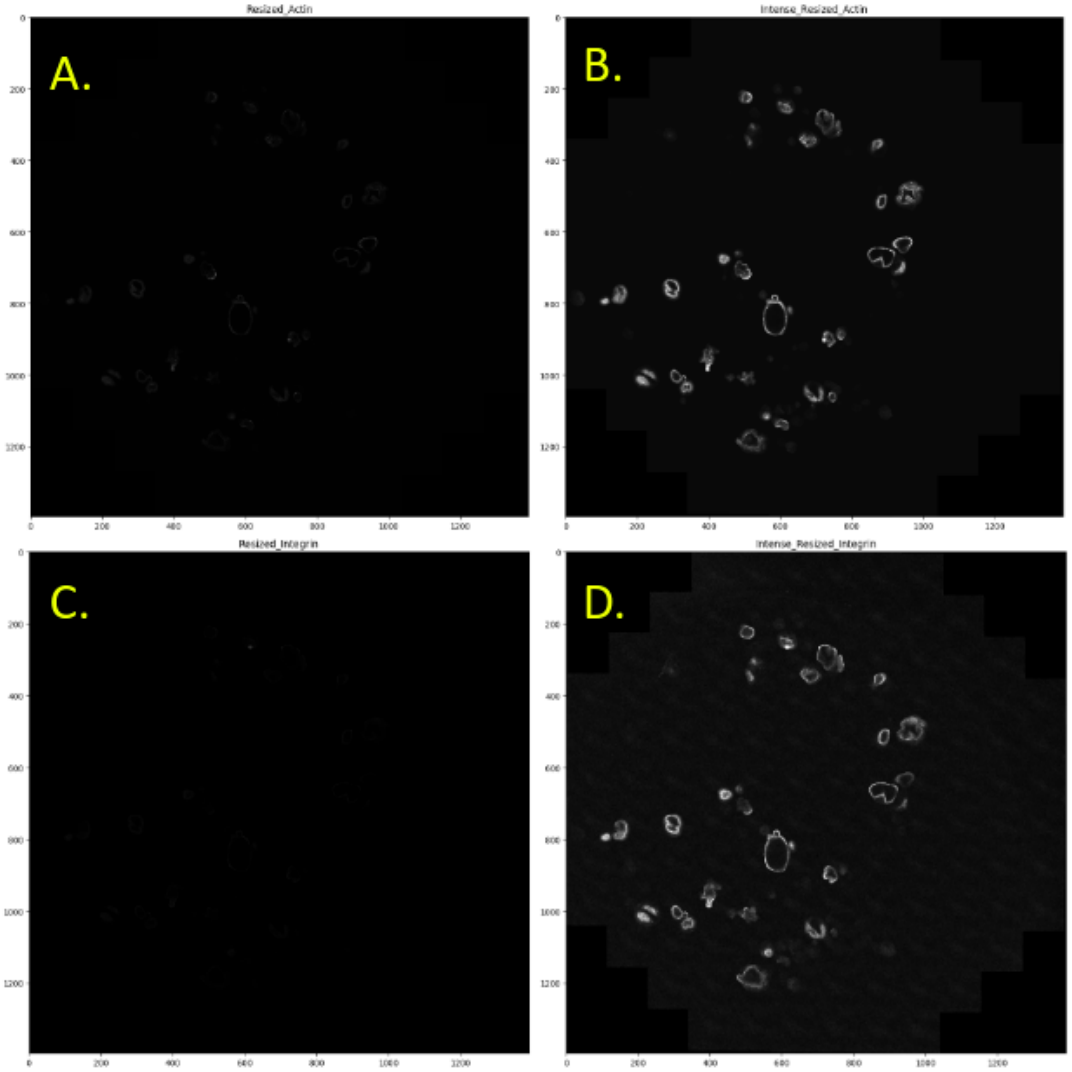

Figure 25. Showing the RescaleIntesity module. (A) F-actin image before rescaling (B) F-actin image after rescaling (C) a6-integrin image before rescaling (D) a6-integrin image after rescaling

Quantification of organoids

In normal intestinal organoids, the integrin is expressed on the outer membrane of the organoids. While in inverted organoids, the actin is on the outer membrane. This difference is used to identify whether an organoid is normal or inverted.

IdentifyPrimaryObjects

First, all Integrin bodies are identified. using IdentifyPrimaryObjects (Figure 26). IdentifyPrimaryObjects module is used with advanced settings. For some parameters the default settings of this module are used, only the exemptions are listed. The typical diameter of the integrin bodies is between 20 and 200 pixels. Objects outside this diameter range and objects toucher the border are discarded. A global 2-class Otsu method is used for thresholding. A correction factor of 0.5 is applied. The declumping of objects and drawing of dividing lines are both based on the shape of the object.

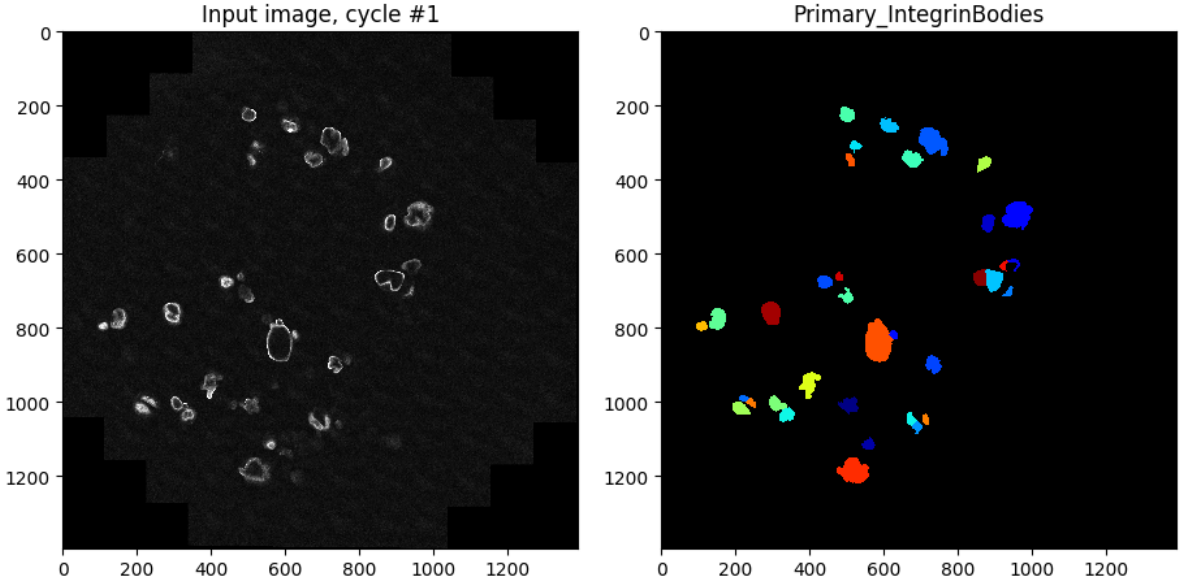

Figure 26. Showing the IdentifyPrimaryObjects module. On the left is the original integrin image. On the right are the identified objects.

These objects are used in order to identify inversed organoids. These objects are subtracted from the F-actin image. All normal organoids will be removed because the integrin object is on the outside of the organoids and thus is larger. While all inverted organoids will still be present. Here the F-actin ring is larger than the integrin ring, thus subtracting the integrin signal from the actin signal will result in actin rings.

ExpandOrShrinkObjects

Because after subtraction of the integrin object, the inverse actin signal should still form a full circle, the integrin objects are shrunken by 2 pixels. With this method, all pixels on the perimeter of the object are removed twice, thus on all sides, the object is 2 pixels smaller.

MaskImages

The shrunken integrin objects are used as a mask for the actin image. The mask is inverted, this results in the original actin image where all integrin objects are blacked out (figure 27). This image can be used to identify all organoids where the actin ring is on the outside of the integrin bodies.

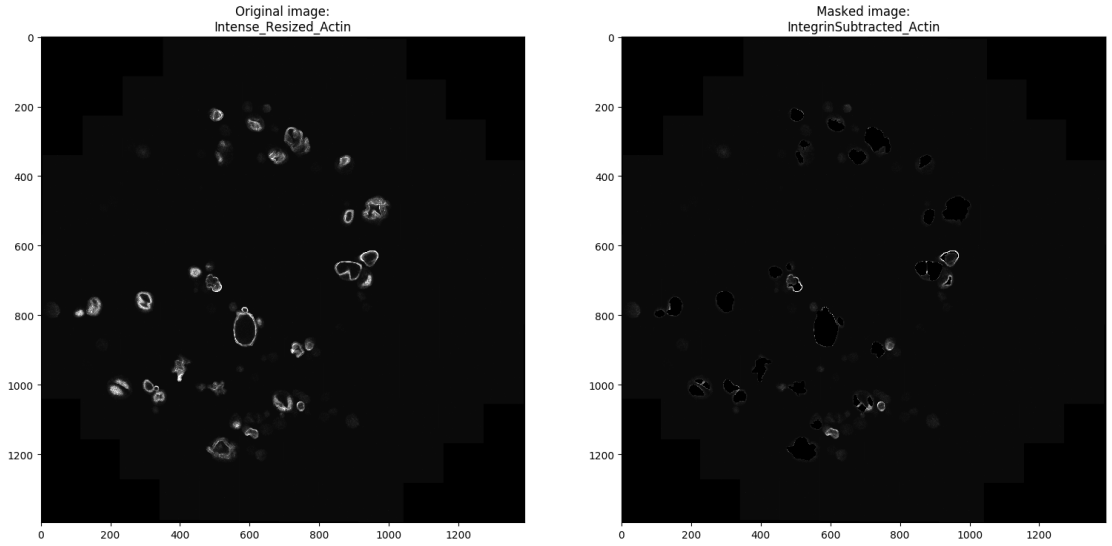

Figure 27. The results of the MaskImages module. On the left, the original actin image, on the right the actin image with the integrin objects blacked out.

IdentifyPrimaryObjects

The IdentifyPrimaryObjects module is used on the masked actin image, to quantify all inversed organoids (figure 28). The IdentifyPrimaryObjects module is used with advanced settings. For some parameters the default settings of this module are used, only the exemptions are listed. The typical size of the inverted organoids is between 20 and 100 pixels. object touching the border of the image is not discarded. A manual thresholding method is selected and set to 0.15. The declumping of objects and drawing of dividing lines are both based on the shape of the object.

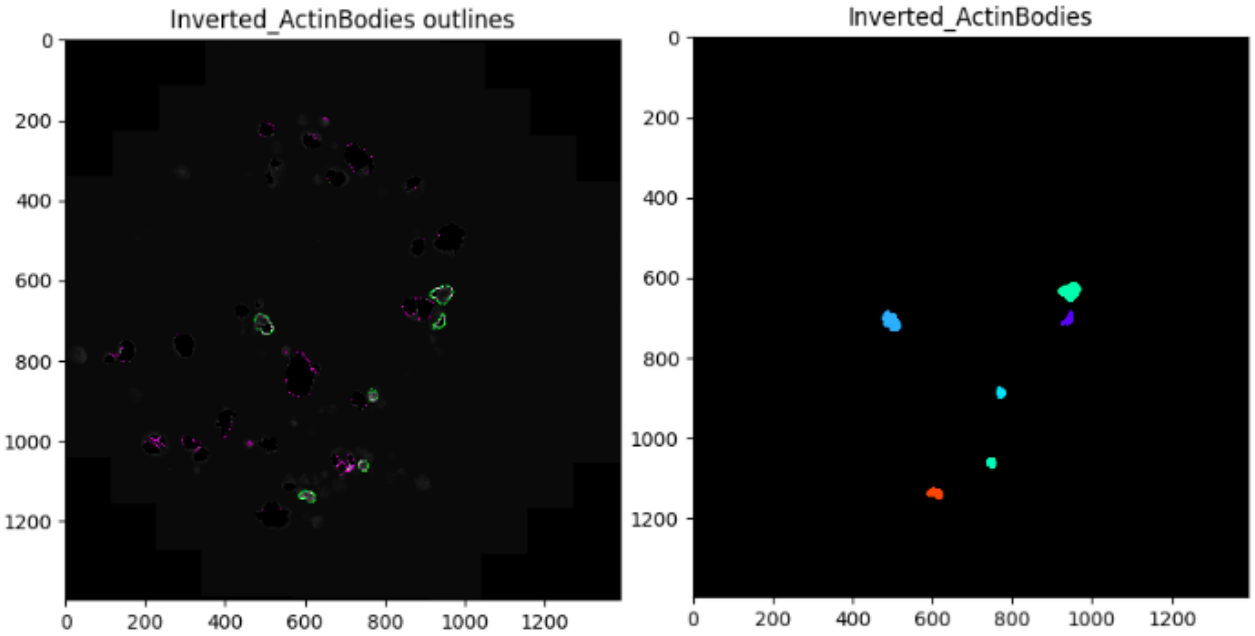

Figure 28. Showing the accepted and denied objects in the masked actin image. On the left are the objects found in the original image, green outlined objects are accepted, magenta outlined objects are denied due to size. On the right are the generated objects.

ExpandOrShrinkObjects

In order to further identify all normal organoids, the inverse objects that have been found are enlarged. These enlarged objects can then be used to remove the inverse organoids from the actin signal. To enlarge the object, one pixel is added to each pixel that is on the outside of an object. This process is repeated 15 times for every

object, thus adding 15 pixels to every possible side of each found object.

MaskImages

The enlarged objects based on the inversed organoids are used to mask the actin image. The mask is inverted thus resulting in an image where all normal organoids are showing. And all organoids that are inverted are blacked out (figure 29).

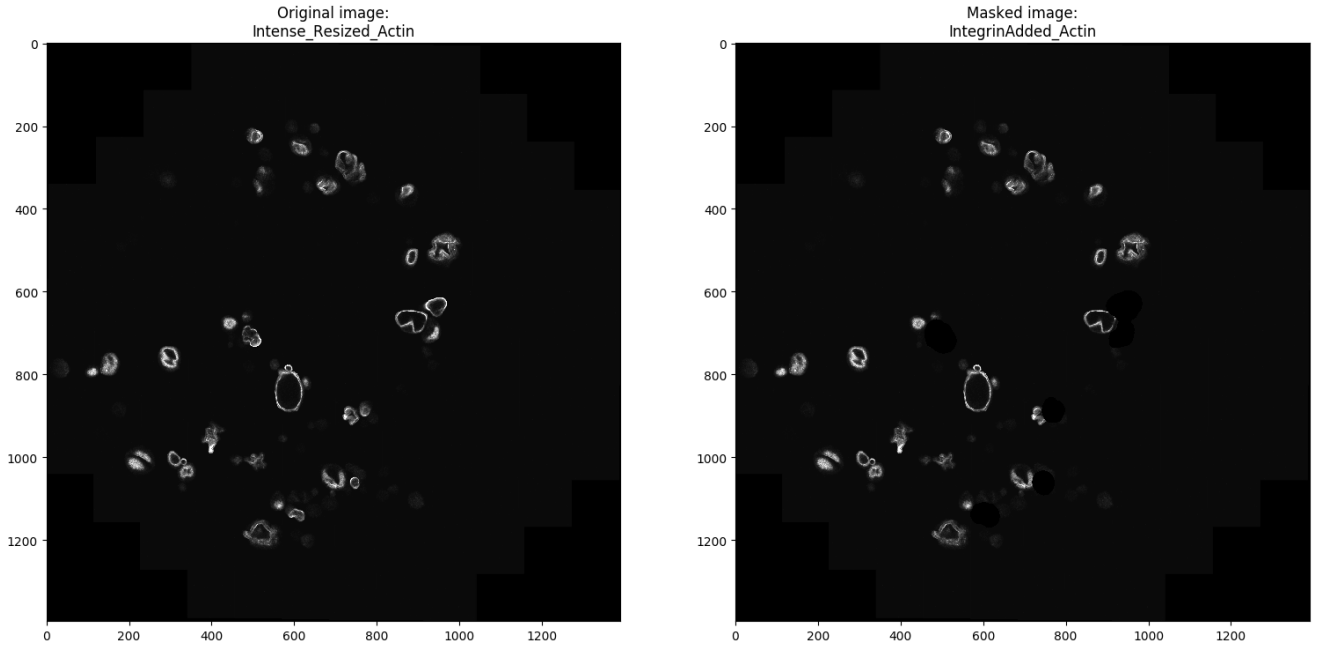

Figure 29. Showing the MaskImages module. On the left, the original actin staining. On right the masked image, showing blacked-out spots where the inverted organoids are.

IdentifyPrimaryObjects

The IdentifyPrimaryObjects module is used on the masked actin image, to quantify all normal organoids (figure 30). The IdentifyPrimaryObjects module is used with advanced settings. For some parameters the default settings of this module are used, only the exemptions are listed. The typical diameter of the organoids is between 20 and 100 pixels. All objects touching the border of the image are retained. A global manual threshold is selected and set to 0.15. The declumping of objects and drawing of dividing lines are both based on the shape of the object.

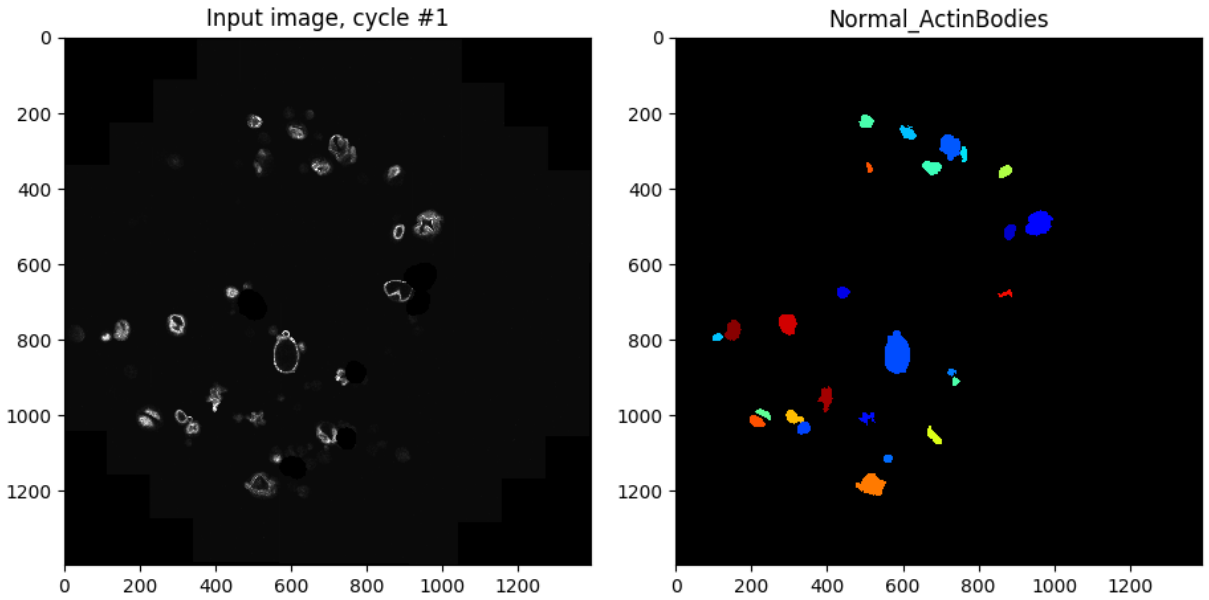

Figure 30. Showing the IdentifyPrimaryObjects module. On the left is the masked actin image. On the right, the identified and accepted objects.

Result image generation

Resize

In order to project the quantification of the organoids, the original image needs to be resized as well. Thus the image generated in the GrayToColor module is shrunken to 25% of its initial size.

DisplayDataOnImages

The module is used twice in order to project the counted organoids over the original image. Showing both normal and inverted organoids (figure 31).

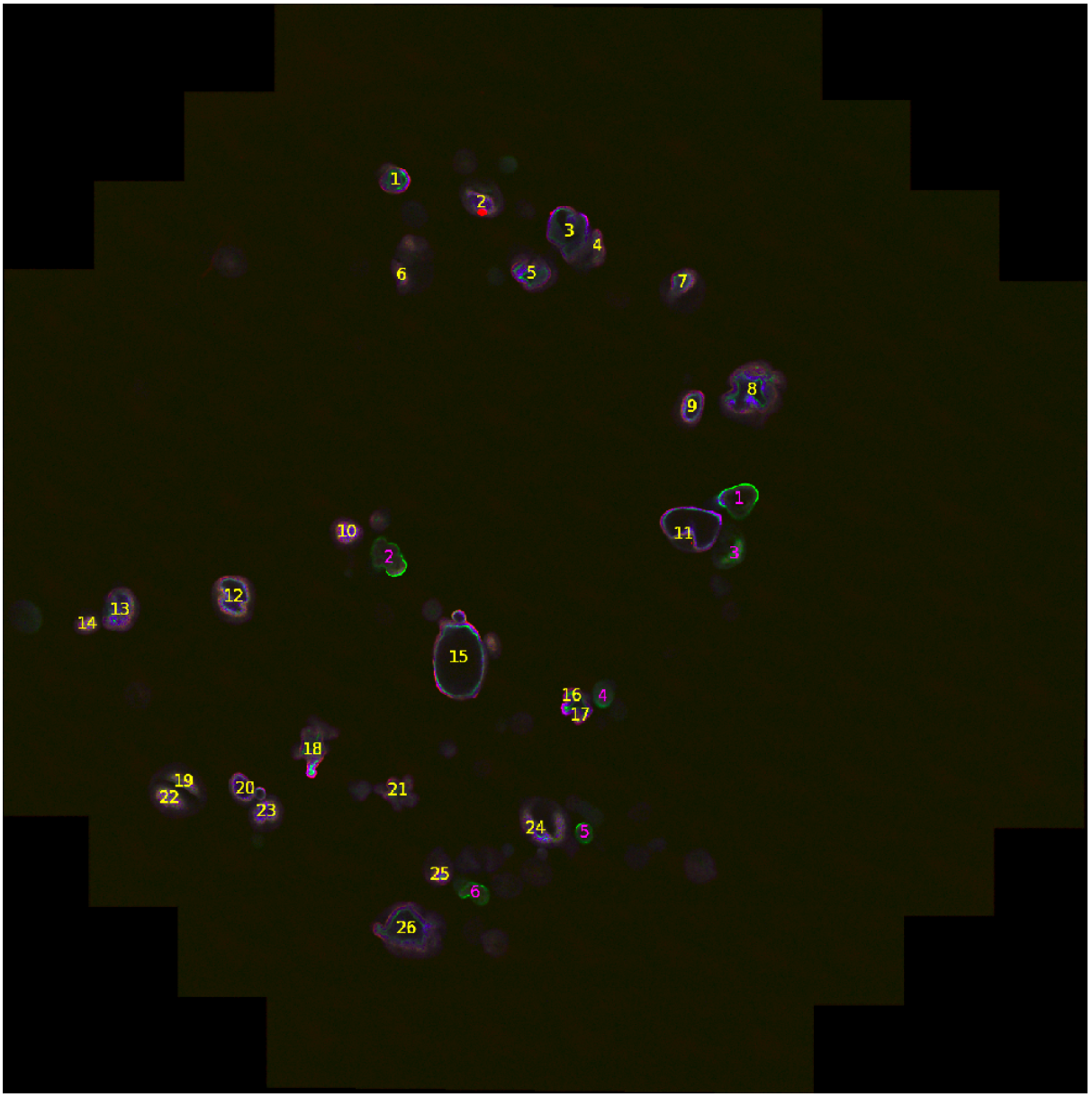

Figure 31. Showing the results from the pipeline. Both normal organoids (yellow) and inverted organoids (Magenta) are quantified in the same image.

SaveImages

The image from the last module is saved in a custom output location.

Results

The goal of the project is to set up a pipeline that is capable of separating both normal and inverted organoids. Cellprofiler4.0 finds more normal organoids than that there are in the images in all cases (N=5). While Cellprofiler4.0 correctly finds all inverse organoids in 2 cases while in 3 cases Cellprofiler4.0 finds fewer inverse organoids than there are in the image (table 8).

Table 8. comparing the number of organoids found by Cellprofiler4.0 and by counting organoids by hand. accuracy is calculated by adding correctly classified sites and dividing it by the total number of reference sites.

	Hand count		**Cellprofiler4.0**		**Cellprofiler4.0 sensitivity**	
Image	**Normal**	**Inversed**	**Normal**	**Inversed**	**Normal**	**Inversed**
1	30	3	37	2	1.233	0.666
2	20	3	30	2	1.500	0.666
3	15	3	16	3	1.066	1
4	17	3	27	2	1.588	0.666
5	23	6	26	6	1.130	1

Discussion

The Cellprofiler4.0 pipeline is quite good at distinguishing inverse organoids from normal organoids. But the pipeline needs some improvement in segmenting and declumping large organoids. Currently, Cellprofiler4.0 finds more normal organoids than when organoids are counted by hand. This can be blamed on the declumping. If large groups of organoids grow closer to each other, Cellprofiler4.0 has more difficulties separating them correctly. As can be observed in image 4 (table 8). Where Cellprofiler4.0 finds 10 organoids to many. This image contains a large cluster of closely growing organoids, which Cellprofiler4.0 finds very hard to separate (Figure 32). This results in single organoids being recognized and counted as several organoids. Although the separation between

inverse and normal organoids works well. The quantification within these separated groups can be highly optimized.

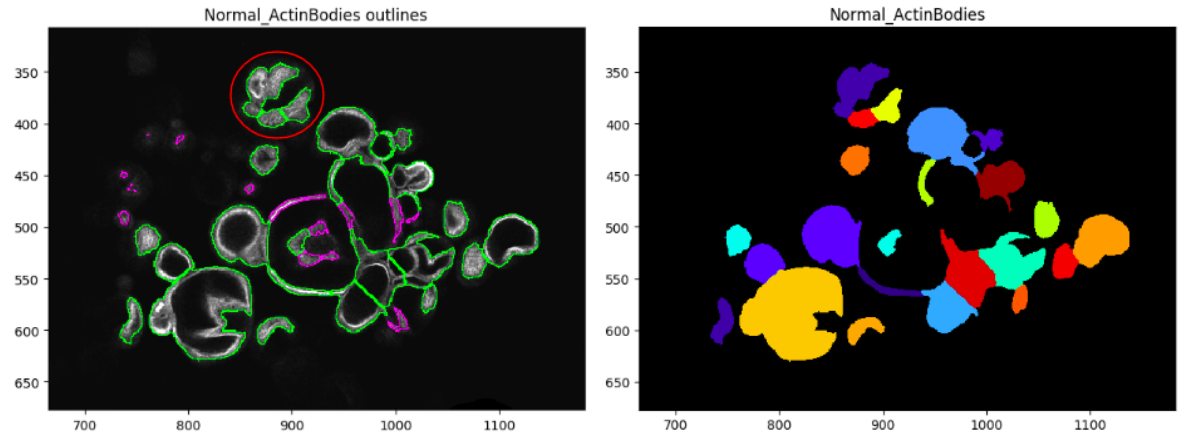

Figure 32. Showing a zoomed-in view on a group of organoids. Cellprofiler4.0 wrongly counts single organoids as multiple organoids. In an example in the left panel within the red circle.

Besides normal polarization and inverted polarization, the intestinal organoids can exist in a third state. This state is called aberrant.

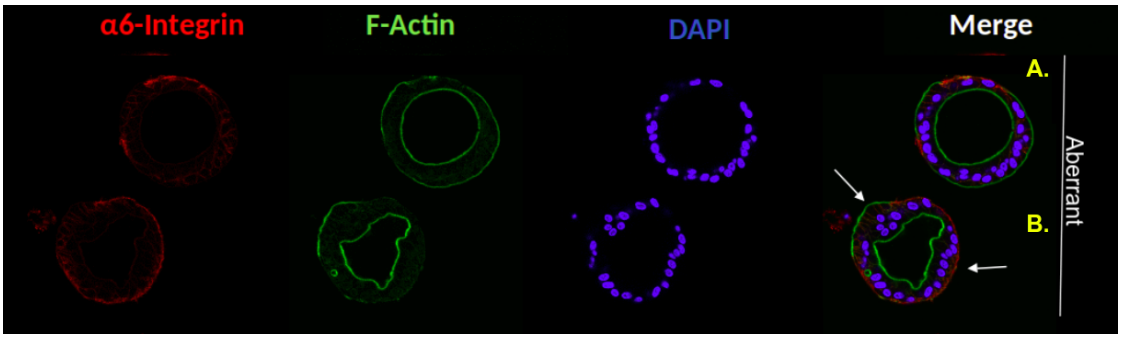

Figure 33. Showing the expression of a6-integrin (red), F-actin (green), and DNA (DAPI) within organoids with aberrant polarity. (A) showing an example of an organoid have F-actin and a6-integrin expressed both in the outer lumen. (B) Showing an example of F-actin lining multiple lumens

Aberrant polarity is assigned to organoids that show expression of both α6-Integrin and F-actin at their outer border (figure 33A), to organoids with multiple F-actin-lined lumens (figure 33B), and also to organoids that completely lack the expression of either α6-Integrin or F-actin. We tried to use Cellprofiler to extract these forms of polarization as well, but sadly it didn't work. The structural

differences with normally polarized organoids are too small for Cellprofiler to differentiate. Background staining is also seen in these images. This background staining obstructs the identification of organoids. Cellprofiler has difficulties with distinguishing the background noise from the organoids because the intensity differences are too small.

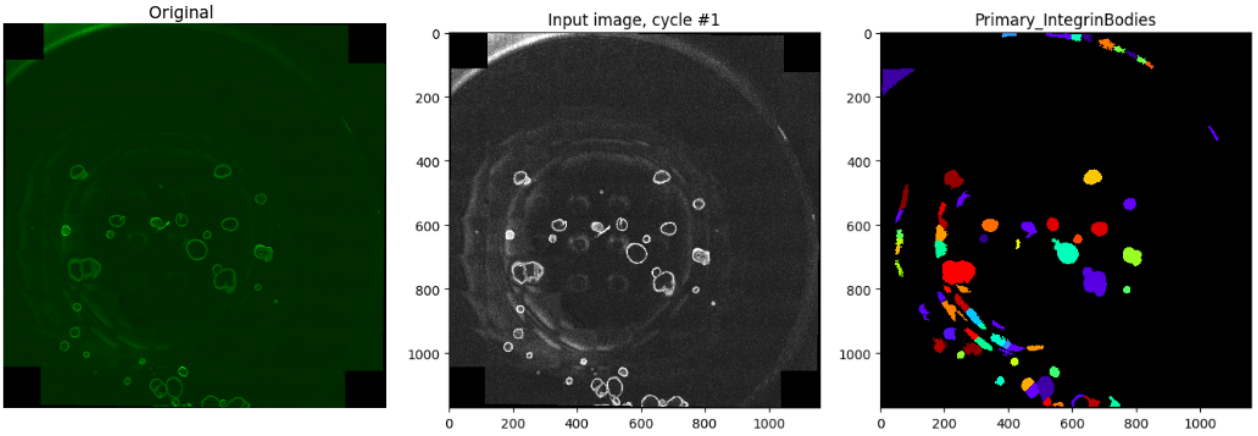

Figure 34. Showing the original integrin staining, conversion to black and white, and the identifyPrimaryObjects module. in the original integrin staining (left) a lot of background staining is observed. The background noise is also observed when the image is converted to black and white (middle). This results in a lot of false positives within the identifyPrimaryObjects module of cellprofiler (right)

Overall conclusion

The aim of this study was to investigate the flexibility of Cellprofileras a platform to analyze real-life image analysis from human material (disease stage) generated by various researchers. Here we describe how Cellprofiler can be used to:

- ➢ Analyze nuclei size in primary cardiac tissue;
- ➢ Differentiate nuclei based on the cell type in primary cardiac tissue;
- ➢ Analyze the nuclear structure of LMNA KO- and KD-clones in an intestinal organoid model;
- ➢ Differentiate the polarization of membrane layers in intestinal organoids.

Showing Cellprofiler is no black box system. It is giving the analyst the power to correct errors in imaging and emphasizing the importance of close collaboration between imager and analyst.

Table 9.

Cellprofiler4.0 pipelines			
Primary cardiac tissue - PLN	**IPSC-cardiomyocyte model**	**Intestinal organoids - LMNA KO, KD**	**Intestinal organoids - polariy**
IdentifyPrimaryObjects	ColorToGray	ColorToGray	GrayToColor
MaskImage	IdentifyPrimaryObjects	Threshold	Resize
IdentifyPrimaryObjects	DisplayDataOnImage	MaskImage	RescaleItensity
MaskImage	SaveImages	IdentifyPrimaryObjects	Resize
IdentifyPrimaryObjects	MeasureObjectSizeShape	DisplayDataOnImage	RescaleIntensity
GrayToColor	ExportToSpreadsheet	SaveImages	IdentifyPrimaryObjects
DisplayDataOnImage		MeasureObjectSizeShape	ExpandOrShrinkObjects
DisplayDataOnImage		ExportToSpreadshet	MaskImages
SaveImages			IdentifyPrimaryObjects
MeasureObjectSizeShape			ExpandOrShrinkObjects
ExportToSpreadsheet			MaskImages
			IdentifyPrimaryObjects
			Resize
			DisplayDataOnImages
			DisplayDataOnImages
			SaveImages

Overall discussion

Cellprofiler is a really powerful piece of software. It is capable of analyzing primary cells, scans, organoids, and even tissue. Cellprofiler can be very precise but lacks some power in correcting the images. The better the microscopy images are the better Cellprofiler works. Although Cellprofiler can in for example, correct for holes in the tissue, as seen in the sacromeres in the nuclei differentiation pipeline. If the holes are too big, as seen in the same

pipeline with the nuclei itself, it is not as precise anymore. The same goes for background lighting, if there is too much background staining, Cellprofiler has large difficulties to differentiate foreground and background, as seen in the organoid polarization pipeline.

Acknowledgments

I would like to thank the whole Harakalova/v. Steenbeek group for setting this project up and helping me throughout. Special thanks to my supervisor Magdalena Harakalova for the personal guidance. And to Michal Mokry, Bianca A. Meyers, Christian Snijders-Blok, Renee Maas, Maaike de Vries and Zahra Shojaeijeshvaghani for providing me with data I could analyse.

Additional

When running Cellprofiler locally, one could run into some problems. Because microscopy images can get quite large, the usage of Cellprofiler can take up quite some memory. In order to tackle this, instead of running Cellprofiler locally, Cellprofiler can be run externally on large servers. One of those servers is Galaxy, which introduces Cellprofiler on July 1st, 2020. The Galaxy instance Europe is the biggest in Europe and has free storage capabilities up to 250 GB for free. The servers can be used to run Cellprofiler without worrying about memory. Together with Niels Mol, we aimed to set up Galaxy as the most used

Supplementary figures

Supplementary figures are added in a separate folder.

References

1. Lay, J. O., Liyanage, R., Borgmann, S. & Wilkins, C. L. Problems with the 'omics'. *Trends Analyt. Chem.* **25**, 1046–1056 (2006).
2. Lander, E. S. The new genomics: global views of biology. *Science* **274**, 536–539 (1996).
3. Idle, J. R. & Gonzalez, F. J. Metabolomics. *Cell Metab.* **6**, 348–351 (2007).
4. Gawad, C., Koh, W. & Quake, S. R. Single-cell genome sequencing: current state of the science. *Nat. Rev. Genet.* **17**, 175–188 (2016).
5. Schueder, F. *et al.* Multiplexed 3D super-resolution imaging of whole cells using spinning disk confocal microscopy and DNA-PAINT. *Nat. Commun.* **8**, 2090 (2017).
6. Kapuscinski, J. DAPI: a DNA-specific fluorescent probe. *Biotech. Histochem.* **70**, 220–233 (1995).
7. Abràmoff, M. D., Magalhães, P. J. & Ram, S. J. Image processing with ImageJ. *Biophotonics international* **11**, 36–42 (2004).
8. Sommer, C., Straehle, C., Köthe, U. & Hamprecht, F. A. Ilastik: Interactive learning and segmentation toolkit. in *Biomedical Imaging: From Nano to Macro, 2011 IEEE International Symposium on* vol. 2011 230–233 (unknown, 2011).
9. Stirling, D. R. *et al.* CellProfiler 4: improvements in speed, utility and usability. *BMC Bioinformatics* **22**, 433 (2021).
10. van den Dungen4 Nico Lansu4 Marc P. Buijsrogge1 Nicolaas de Jonge1 Hester M. den Ruijter1 Gerard Pasterkamp1 Manon M. Huibers5 Roel A. de Weger5 Linda van Laake1 Marianne Verhaar23 Peter van Tintelen1 Frank G. van Steenbeek127 Alain van Mil12 Jan Willem Buikema1 Boudewijn Burgering8 Ioannis Kararikes6 Mark Mercola6 Pieter A. Doevendans19 Joost Sluijter12 Aryan Vink5 Caroline Cheng23 Michal Mokry2410* Folkert W. Asselbergs191112*# Magdalena Harakalova12*#, I. P. R. M. E. N. J. M. I. H.

G. C. S. B. I. van A. J. C. R. van E. S. S. D. F. N. Epigenetic profiling reveals disrupted lipid metabolism in failing hearts and iPSC-cardiomyocytes with a pathogenic phospholamban R14del mutation.

11. Meyer, B. A. Cardiac meets Intestine Establishing a New Model System to Study Cardiomyopathy. (2021).
12. van Opbergen, C. J. M., Delmar, M. & van Veen, T. A. B. Potential new mechanisms of pro-arrhythmia in arrhythmogenic cardiomyopathy: focus on calcium sensitive pathways. *Neth. Heart J.* **25**, 157–169 (2017).
13. Eijgenraam, T. R. *et al.* The phospholamban p.(Arg14del) pathogenic variant leads to cardiomyopathy with heart failure and is unreponsive to standard heart failure therapy. *Sci. Rep.* **10**, 9819 (2020).
14. van der Zwaag, P. A. *et al.* Phospholamban R14del mutation in patients diagnosed with dilated cardiomyopathy or arrhythmogenic right ventricular cardiomyopathy: evidence supporting the concept of arrhythmogenic cardiomyopathy. *Eur. J. Heart Fail.* **14**, 1199–1207 (2012).
15. Kimura, Y. & Inui, M. Reconstitution of the Cytoplasmic Interaction between Phospholamban and Ca2 -ATPase of Cardiac Sarcoplasmic Reticulum. *Molecular Pharmacology* vol. 61 667–673 (2002).
16. Sommariva, E. *et al.* Oxidized LDL-dependent pathway as new pathogenic trigger in arrhythmogenic cardiomyopathy. *EMBO Mol. Med.* **13**, e14365 (2021).
17. Morales, A. *et al.* Late onset sporadic dilated cardiomyopathy caused by a cardiac troponin T mutation. *Clin. Transl. Sci.* **3**, 219–226 (2010).
18. Merritt, J. L., 2nd, Norris, M. & Kanungo, S. Fatty acid oxidation disorders. *Ann Transl Med* **6**, 473 (2018).
19. Syrris, P. *et al.* Clinical expression of plakophilin-2 mutations in familial arrhythmogenic right ventricular cardiomyopathy. *Circulation* **113**, 356–364 (2006).
20. van Tintelen, J. P. *et al.* Plakophilin-2 mutations are the major determinant of

familial arrhythmogenic right ventricular dysplasia/cardiomyopathy. *Circulation* **113**, 1650–1658 (2006).

21. Lee, J. *et al.* Activation of PDGF pathway links LMNA mutation to dilated cardiomyopathy. *Nature* **572**, 335–340 (2019).
22. Yoshida, S., Miwa, H., Kawachi, T., Kume, S. & Takahashi, K. Generation of intestinal organoids derived from human pluripotent stem cells for drug testing. *Sci. Rep.* **10**, 5989 (2020).